

Quantum dynamics and entanglement of a 1D Fermi gas released from a trap

Ettore Vicari

Dipartimento di Fisica dell'Università di Pisa and INFN, Pisa, Italy

We investigate the entanglement properties of the nonequilibrium dynamics of one-dimensional noninteracting Fermi gases released from a trap. The gas of N particles is initially in the ground state within hard-wall or harmonic traps, then it expands after dropping the trap. We compute the time dependence of the von Neumann and Rényi entanglement entropies and the particle fluctuations of spatial intervals around the original trap, in the limit of a large number N of particles. The results for these observables apply to one-dimensional gases of impenetrable bosons as well.

We identify different dynamical regimes at small and large times, depending also on the initial condition, whether it is that of a hard-wall or harmonic trap. In particular, we analytically show that the expansion from hard-wall traps is characterized by the asymptotic small-time behavior $S \approx (1/3) \ln(1/t)$ of the von Neumann entanglement entropy, and the relation $S \approx \pi^2 V/3$ where V is the particle variance, which are analogous to the equilibrium behaviors whose leading logarithms are essentially determined by the corresponding conformal field theory with central charge $c = 1$.

The time dependence of the entanglement entropy of extended regions during the expansion from harmonic traps shows the remarkable property that it can be expressed as a global time-dependent rescaling of the space dependence of the initial equilibrium entanglement entropy.

PACS numbers: 03.65.Ud, 05.30.Fk, 67.85.-d

I. INTRODUCTION

The recent progress in the experimental activity in atomic physics, quantum optics and nanoscience has provided a great opportunity to investigate the interplay between quantum and statistical behaviors in particle systems. The great ability in the manipulation of cold atoms [1–3] allows the realization of physical systems which are accurately described by theoretical models such as dilute atomic Fermi and Bose gases, Hubbard and Bose-Hubbard models, with different effective spatial dimensions from one to three, achieving through experimental checks of the fundamental paradigm of the condensed matter physics. Experiments of cold atoms in optical lattices have provided a great opportunity to investigate the unitary quantum evolution of closed many-body systems, exploiting their low dissipation rate which maintains phase coherence for a long time [3, 4]. In this experimental context, the theoretical investigation of nonequilibrium dynamics in quantum many-body systems, and the time evolution of the entanglement properties characterizing the quantum correlations, is of great importance for a deep understanding of the fundamental issues of quantum dynamics, their possible applications, and new developments.

We consider the nonequilibrium quantum dynamics of particle systems which are initially trapped within a limited region of space by an external force, and then released from the trap. Interesting cases are Fermi gases, or Bose gases with repulsive interactions, which are initially confined within hard-wall or harmonic traps. The free expansion of gases after the drop of the trap is routinely exploited in experiments to infer the properties of the initial quantum state of the particles within the trap [3], observing the interference patterns of absorption images in the large-time ballistic regime. The time-dependence

of the particle density and correlations have been investigated in the literature, see, e.g., Refs. [3, 5–11]. In this paper we focus on the time evolution of the entanglement properties, and their relations with other quantum correlations. Our study should provide further information to the general issue of the entanglement properties in nonequilibrium dynamics after quantum quenches, which have recently attracted much interest; they have been investigated in various models, and for various global and local quenching mechanisms, see, e.g., Refs. [12–22].

The quantum correlations arising during the nonequilibrium many-body dynamics can be characterized by the expectation values of product of local one-particle operators, such as the particle density, the one-particle and density correlations, etc..., or by their integral over a space region A , such as the cumulants of the particle-number distribution within A [19, 23–27]. Quantum correlations are also characterized by the fundamental phenomenon of entanglement, which gives rise to nontrivial connections between different parts of extended quantum systems [12, 13, 28, 29]. A measure of entanglement is achieved by computing von Neumann (vN) or Rényi entanglement entropies of the reduced density matrix of a subsystem. One-particle correlations and bipartite entanglement entropies provide important and complementary information of the quantum behavior of many-body systems, of their ground states (in particular in connection with critical behavior) and of their nonequilibrium unitary evolutions under time variations of the Hamiltonian, because they probe different features of the quantum dynamics.

In this paper we consider a one-dimensional (1D) noninteracting Fermi gas of N particles whose initially zero-temperature state is the ground state within hard walls or in the presence of an external harmonic potential. This model has a wider application, because 1D Bose

gases in the limit of strong short-ranged repulsive interactions can be mapped into a spinless fermion gas, see, e.g., Ref. [30]. Indeed, 1D Bose gases with repulsive two-particle short-ranged interactions, described by the Lieb-Liniger model [31], become more and more nonideal with decreasing the particle density, acquiring fermion-like properties, so that the 1D gas of impenetrable bosons, or Tonks-Girardeau gas [32], provides an effective description of the low-density regime of 1D bosonic gases [33]. Due to their exact mapping, 1D gases of impenetrable bosons and spinless fermions share the same quantum correlations related to the particle density, particle fluctuations of extended regions, and bipartite entanglement entropies of connected parts, even during nonequilibrium dynamics. 1D systems are investigated experimentally, indeed the possibility of tuning the confining potential in experiments allows to vary the effective spatial geometry of the particle systems, realizing quasi-1D geometries of trapped quantum gases, see, e.g., Refs. [34–39].

We study the quantum correlations of the 1D Fermi gas of N particles after the instantaneous drop of the trap, or during a change of the harmonic potential. We focus on their large- N limit, which turns out to be rapidly approached with increasing N . In order to characterize the entanglement properties, we study the time dependence of the entanglement entropy of extended regions in proximity to the initial trap. We show that some regimes of the time evolution are characterized by asymptotic behaviors analogous to the equilibrium (ground-state) ones, whose leading logarithms are essentially determined by the corresponding conformal field theory with central charge $c = 1$. Moreover, we investigate the relations between entanglement entropies and the distribution of the particle number within the same extended region. In the ground state of noninteracting Fermi gases the entanglement entropies are asymptotically proportional to the particle variance for a large number of particles [27, 40]. Thus the particle variance may be considered as an effective probe of entanglement in these class of systems, which should be more easily accessible to experiments. We show that this feature of the ground state of noninteracting Fermi gases is maintained in some regimes of the nonequilibrium dynamics after the gas is released from the trap. In the case of harmonic traps, the time dependence of the entanglement properties during the expansion of the Fermi gas shows the remarkable property that it can be expressed as a global time-dependent rescaling of the initial equilibrium space dependence.

The paper is organized as follows. In Sec. II we report the many-body wave function describing the free expansion of a Fermi gas of N particles from hard-wall traps, and define the observables we consider. In Sec. III we determine the large- N time evolution of several observables, and in particular of the entanglement entropies and particle fluctuations of extended regions around the initial trap. In Sec. IV we consider alternative large- N limits, keeping Nt or N^2t fixed, to study the small-time behaviors, i.e. for $t \sim 1/N$ and $t \sim 1/N^2$, which are

characterized by other scaling behaviors. Sec. V considers the case of a Fermi gas which expands after only one wall drops instantaneously, thus expanding along only one direction. In Sec. VI we study the nonequilibrium evolution of Fermi gases in a time-dependent confining harmonic potential, and in particular after the instantaneous drop of the harmonic trap. Finally, in Sec. VII we summarize our main results and draw our conclusions.

II. MANY-BODY WAVE FUNCTION AND OBSERVABLES

A. Free expansion from hard-wall traps

1. Both walls drop

We consider a gas of N spinless noninteracting fermionic particles of mass m , within a hard-wall trap of size $[-l, l]$. We set $\hbar = 1$, $m = 1$ and $l = 1$, so that time is measured in unit of ml^2/\hbar .

At $t = 0$ the system is in its ground state, whose many-body wave function is

$$\Psi(x_1, \dots, x_N; t = 0) = \frac{1}{\sqrt{N!}} \det[\phi_i(x_j)] \quad (1)$$

where $\phi_k(x)$ are the N lowest eigenstates of the free one-particle Schrödinger problem with boundary conditions $\phi_k(-1) = \phi_k(1) = 0$, i.e.

$$\phi_k(x) = \sin\left[\frac{\pi}{2}k(1+x)\right], \quad e_k = \frac{\pi^2}{8}k^2, \quad k = 1, 2, \dots \quad (2)$$

The free expansion of the gas after the instantaneous drop of the walls is described by the time-dependent wave function

$$\Psi(x_1, \dots, x_N; t) = \frac{1}{\sqrt{N!}} \det[\psi_i(x_j, t)] \quad (3)$$

where $\psi_i(x, t)$ are the one-particle wave functions with initial condition $\psi_i(x, 0) = \phi_i(x)$, which can be written using the free propagator P as

$$\psi_i(x, t) = \int_{-1}^1 dy P(x, t; y, 0) \phi_i(y), \quad (4)$$

$$P(x_2, t_2; x_1, t_1) = \frac{1}{\sqrt{i2\pi(t_2 - t_1)}} \exp\left[\frac{i(x_2 - x_1)^2}{2(t_2 - t_1)}\right].$$

Note that they have a definite parity $P_k = (-1)^{k-1}$. Eq. (4) can also be written as

$$\begin{aligned} \psi_n(x, t) &= \frac{e^{ix^2/(2t) + in\pi/2}}{2i\sqrt{i2\pi t}} [f_n(x, t) + (-1)^{1+n} f_n(-x, t)], \\ f_n(x, t) &= \int_{-1}^1 dy \exp\left[i\frac{y^2}{2t} - iy\left(\frac{x}{t} - \frac{\pi n}{2}\right)\right]. \end{aligned} \quad (5)$$

This integral can be expressed in terms of the complementary error function or the Fresnel functions, see, e.g., Refs. [41, 42].

2. Only one wall drops

We also consider the case of a gas expanding after the instantaneous drop of only one of the walls. For simplicity, we consider an initial trap of size $[0, l]$. We again set $l = 1$. Then, after the instantaneous drop of the hard wall at $l = 1$, the gas expands along the positive real axis. In this case the one-particle eigenstates of the system at $t = 0$ are

$$\phi_k(x) = \sqrt{2} \sin(\pi k x), \quad e_k = \frac{\pi^2}{2} k^2, \quad k = 1, 2, \dots \quad (6)$$

The evolution of the wave function $\psi_i(x, t)$ for $t > 0$ requires the appropriate propagator Q which ensure the boundary condition $\psi_k(0, t) = 0$, i.e.

$$\psi_k(x, t) = \int_0^1 dy Q(x, t; y, 0) \phi_k(y), \quad (7)$$

$$Q(x_2, t_2; x_1, t_1) = P(x_2, t_2; x_1, t_1) - P(-x_2, t_2; x_1, t_1).$$

B. Observables

The equal-time two point function, the particle density and its correlation function can be written in terms of the one-particle wave functions $\psi_n(x, t)$,

$$C(x, y, t) \equiv \langle c^\dagger(x, t) c(y, t) \rangle = \sum_{i=1}^N \psi_i(x, t)^* \psi_i(y, t), \quad (8)$$

$$\rho(x, t) \equiv \langle n(x, t) \rangle = C(x, x, t) = \sum_{i=1}^N |\psi_i(x, t)|^2, \quad (9)$$

$$G_n(x, y, t) \equiv \langle n(x, t) n(y, t) \rangle_c = -|C(x, y, t)|^2 + \delta(x - y) C(x, y, t), \quad (10)$$

where $c(x, t)$ is the time-dependent fermionic annihilation operator and $n(x, t) = c(x, t)^\dagger c(x, t)$ is the particle-density operator.

Other interesting measures of the quantum correlations are related to extended spatial regions, where we may consider the time-dependent distribution of the particle number and the entanglement with the rest of the system. In the following, we consider extended intervals $A = [x_1, x_2]$ with x_1, x_2 of the size of the initial trap. For example, one may just consider the interval corresponding to the initial trap $[-1, 1]$.

We consider the particle-number operator of an extended region A

$$\hat{N}_A(t) = \int_A dx n(x, t). \quad (11)$$

Its expectation value and connected correlation function, respectively

$$N_A = \langle \hat{N}_A \rangle, \quad \langle \hat{N}_A^m \rangle_c = \int_A \prod_{i=1}^m d^d x_i \langle \prod_{i=1}^m n(\mathbf{x}_i) \rangle_c, \quad (12)$$

characterize the particle distribution within A . For this purpose, it is convenient to introduce the cumulants of the particle distribution, which can be defined through a generator function as [43]

$$V_A^{(m)} = (-i\partial_\lambda)^m \ln \langle e^{i\lambda \hat{N}_A} \rangle |_{\lambda=0}. \quad (13)$$

In particular, the particle variance reads

$$V_A \equiv V_A^{(2)} = \langle N_A^2 \rangle - \langle N_A \rangle^2 = \int_A dx dy G_2(x, y, t) \quad (14)$$

(the superscript $m = 2$ will be understood in the case of the particle variance).

A measure of the entanglement of the extended region A with the rest of the system is provided by the Rényi entanglement entropies, defined as

$$S_A^{(\alpha)} = \frac{1}{1 - \alpha} \ln \text{Tr} \rho_A^\alpha \quad (15)$$

where $\rho_A(t)$ is the time-dependent reduced density matrix of the subsystem A . For $\alpha \rightarrow 1$, we recover the vN definition

$$S_A \equiv S_A^{(1)} \equiv -\text{Tr} \rho_A \ln \rho_A \quad (16)$$

(the superscript $\alpha = 1$ will be understood in the case of the vN entanglement entropy).

In noninteracting Fermi gases the particle cumulants and the entanglement entropies of a subsystem A can be related to the two-point function C restricted within A , which we denote by C_A . This fact holds also in nonequilibrium dynamics [13]. The particle number and cumulants within A can be derived using the relations (see e.g. Ref. [26])

$$N_A = \text{Tr} C_A, \quad (17)$$

$$V_A^{(m)} = (-i\partial_z)^m \mathcal{G}(z, C_A) |_{z=0}, \quad (18)$$

$$\mathcal{G}(z, \mathbb{X}) = \text{Tr} \ln [1 + (e^{iz} - 1) \mathbb{X}]. \quad (19)$$

The vN and Rényi entanglement entropies can be also related to the two-point function C_A (see Refs. [13, 44] for applications to lattice systems).

In noninteracting Fermi gases with N particles, the computation of the particle cumulants and entanglement entropies is much simplified by introducing and exploiting the information contained in the $N \times N$ overlap matrix of the one-particle wave functions [45], as shown in the studies of the ground-state entanglement properties of homogenous Fermi gases [46, 47], in the presence of impurities and for quantum wires [48], and in the presence of a space-dependent harmonic trapping potential [40]. As already anticipated in Ref. [45], the method can be extended to nonequilibrium quantum dynamics, by defining the time-dependent overlap $N \times N$ matrix

$$\mathbb{A}_{nm}(t) = \int_A dz \psi_n^*(z, t) \psi_m(z, t), \quad n, m = 1, \dots, N, \quad (20)$$

where the integration is over the spatial region A , and involves the time evolutions $\psi_n(x, t)$ of the lowest N energy states of the one-particle Schrödinger problem at $t = 0$. The overlap matrix \mathbb{A} and the restricted two point function C_A satisfy

$$\text{Tr } C_A^k = \text{Tr } \mathbb{A}^k \quad \forall k \in \mathbb{N}, \quad (21)$$

which implies that the particle cumulants and the entanglement entropies can be computed from the eigenvalues a_i of the $N \times N$ overlap matrix \mathbb{A} , which are real and limited, $a_i \in (0, 1)$. Therefore, the particle number and cumulants can be derived by replacing C_A with \mathbb{A} in Eq. (18). In particular,

$$V_A = \text{Tr} \mathbb{A}(1 - \mathbb{A}), \quad (22)$$

$$V_A^{(3)} = \text{Tr}[\mathbb{A} - 3\mathbb{A}^2 + 2\mathbb{A}^3], \quad (23)$$

$$V_A^{(4)} = \text{Tr}[\mathbb{A} - 7\mathbb{A}^2 + 12\mathbb{A}^3 - 6\mathbb{A}^4], \quad (24)$$

etc.... The vN and Rényi entanglement entropies are obtained by [45]

$$S_A^{(\alpha)} = \sum_{n=1}^N s_\alpha(a_n), \quad (25)$$

where a_n are the eigenvalues of \mathbb{A} , and

$$s_\alpha(\lambda) = \frac{1}{1-\alpha} \ln[\lambda^\alpha + (1-\lambda)^\alpha]. \quad (26)$$

and, in particular,

$$s_1(\lambda) = -\lambda \ln \lambda - (1-\lambda) \ln(1-\lambda) \quad (27)$$

for the vN entropy. We also mention that the determinant of the overlap matrix of a space region A provides the time-dependent probability to find all particles within A [49], indeed

$$\det \mathbb{A} = \int_{A^N} \prod_{i=1}^N dx_i |\Psi(x_1, \dots, x_N; t)|^2 \quad (28)$$

In the following we drop the subscript A in the quantities related to extended regions A .

III. TIME DEPENDENCE FOR A LARGE NUMBER OF PARTICLES

In this section we consider the expansion of the gas from the hard-wall trap $[-1, 1]$, when both walls drop instantaneously, corresponding to the many-body wave function reported in Sec. II A 1. We determine the time evolution of entanglement entropies and particle fluctuations for a large number of particles.

A. The large- N limit

The large- N limit of the equal-time two-point function,

$$C(x, y, t) = \frac{1}{2\pi t} \sum_{k=1}^N \int_{-1}^1 dz_1 dz_2 e^{i(x-z_1)^2/(2t)} \times \\ \times e^{-i(y-z_2)^2/(2t)} \phi_k(z_1) \phi_k(z_2), \quad (29)$$

can be obtained using the completeness relation [50]

$$\sum_{k=1}^{\infty} \phi_k(x) \phi_k(y) = \delta(x-y) \quad (30)$$

of the spectrum of the one-particle Hamiltonian at $t = 0$. We obtain the large- N limit

$$C_\infty(x, y, t) = \frac{\sin[(y-x)/t]}{\pi(y-x)} e^{i(x^2-y^2)/(2t)}. \quad (31)$$

Numerical results at finite N , using Eq. (29), show that $C(x, y, t)$ approaches its large- N limit $C_\infty(x, y, t)$ with $O(1/N)$ corrections for any $t > 0$.

If we are only interested in the traces of integer powers of the restriction C_A of C within an extended region A , Eq. (31) can be simplified dropping the phase, i.e.

$$\text{Tr } C_{\infty, A}^k = \text{Tr } \mathbb{C}_A^k, \quad (32)$$

$$\mathbb{C}_A(x, y, t) \equiv \frac{\sin[(y-x)/t]}{\pi(y-x)}. \quad (33)$$

Note that the above result does not depend on the particular form of the confining potential. The only essential ingredient is that it confines the particles within a strictly finite region of space. For example, the above method to compute the large- N limit fails in the case of a harmonic trap (in this case, after using the completeness relation we would end up with a diverging integral, calling for another approach to get the large- N limit), as we shall see later.

Using Eq. (31), we can easily derive the large- N time evolution of the particle density

$$\rho_\infty(x, t) = C_\infty(x, x, t) = \frac{1}{\pi t}, \quad (34)$$

which means that in the formal large- N limit the particle density is independent of the position. Of course, this regime is approached nonuniformly with respect to the spatial coordinate, but, as we shall see, it is rapidly reached around the central region of the size of the original trap, i.e. $|x| \lesssim 1$.

Let us now consider an extended interval $A = [x_1, x_2]$, with x_i of the size of the original trap. The average number of particles within A is just given by

$$n_\infty(t) = \int_A \rho_\infty(x, t) = \frac{1}{\pi t \delta}, \quad (35)$$

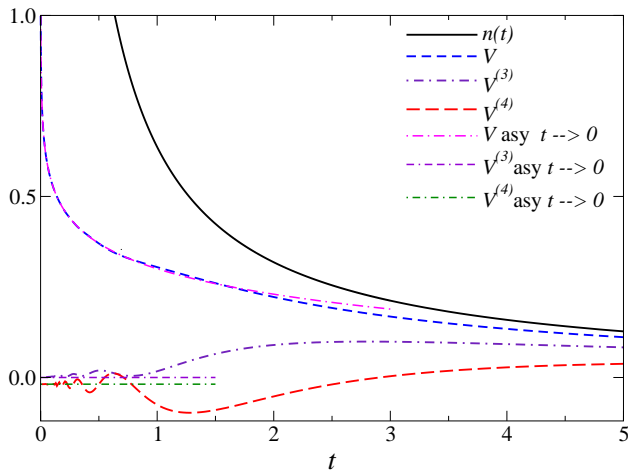


FIG. 1: (Color online) The large- N time dependence of the particle cumulants of the interval $A = [-1, 1]$, and, for comparison, their small- t asymptotic behaviors (49), (51) and (52).

where

$$t_\delta \equiv t/\Delta, \quad \Delta \equiv x_2 - x_1. \quad (36)$$

Large- N corrections are $O(1/N)$. The large- N limit of the particle cumulants can be computed using Eq. (18). For example, the large- N particle variance is obtained by

$$V_\infty(t) = \text{Tr } \mathbb{C}_A(1 - \mathbb{C}_A) = \quad (37)$$

$$= n_\infty(t) - \frac{1}{\pi^2} \int_{x_1}^{x_2} dw_1 dw_2 \left[\frac{\sin(w_1 - w_2)/t}{w_1 - w_2} \right]^2 \quad (38)$$

Analogous, although more cumbersome, expressions can be derived for the higher cumulants, using Eq. (18) with \mathbb{C}_A replaced by \mathbb{C}_A .

In particular, the particle variance of the interval $A = [-1, 1]$, which coincides with the original trap, is given by

$$V_\infty(t) = \frac{2}{\pi t} - \frac{4}{\pi^2 t^2} \left[t \text{Si}(4/t) - \frac{t^2(1 + \gamma_E + \ln(4/t) - \cos(4/t) - \text{Ci}(4/t))}{4} \right] \quad (39)$$

where Ci and Si are the cosine and sine integral functions. At small times the following asymptotic expansion holds

$$V_\infty(t) = \frac{1}{\pi^2} [\ln(2/t) + 1 + \gamma_E + \ln 2] - \frac{\cos(4/t)}{16\pi^2} t^2 \left[1 - \frac{9}{8} t^2 + O(t^4) \right] - \frac{\sin(4/t)}{16\pi^2} t^3 \left[1 - \frac{3}{2} t^2 + O(t^4) \right] \quad (40)$$

In Fig. 1 we show curves for the particle number and the first few cumulants for the interval $A = [-1, 1]$ corresponding to the initial trap.

B. The small- t behavior of bipartite entanglement entropies

The small- t asymptotic behavior of the large- N limit of the entanglement entropies can be analytically computed. For this purpose, we note that the large- N two-point function \mathbb{C}_A , cf. Eq. (33), can be related to an appropriate continuum limit of the lattice two-point function of free fermions. Let us formally discretize the space within $A = [x_1, x_2]$ as

$$y \equiv \frac{i\Delta}{N}, \quad x \equiv \frac{j\Delta}{N}, \quad i, j = 1, \dots, N, \quad (41)$$

where $\Delta = x_2 - x_1$. Then, we consider a discretized version of \mathbb{C}_A , i.e. the $N \times N$ matrix

$$\hat{\mathbb{C}}_A = \frac{N}{\Delta} \frac{\sin[(i-j)\Delta/\tau]}{\pi(i-j)}, \quad \tau \equiv Nt, \quad (42)$$

which is identical to the two-point function of lattice free fermions in the thermodynamic limit without boundaries [13, 44],

$$\mathbb{C}_{ij}^{\text{lat}} = \frac{\sin k_F(i-j)}{\pi(i-j)} \quad (43)$$

(i, j are the lattice sites), replacing the Fermi scale k_F with Δ/τ , and apart from a normalization N/Δ which is the analogue of the inverse lattice spacing, which we may formally set to one. The entanglement entropies of extended regions can be derived from the two-point function only [13]. Using the results of Refs. [44, 51] and the above correspondences, we derive the asymptotic behavior corresponding to Eq. (41), which is

$$S^{(\alpha)} = c_\alpha \left[\ln N + e_\alpha + \ln \sin \frac{\Delta}{\tau} \right] + O(N^{-2/\alpha}) \quad (44)$$

where

$$c_\alpha \equiv \frac{1 + \alpha^{-1}}{6}, \quad (45)$$

$$e_\alpha = \ln 2 + y_\alpha, \quad (46)$$

$$y_\alpha = \int_0^\infty \frac{dt}{t} \left[\frac{6}{1 - \alpha^{-2}} \left(\frac{1}{\alpha \sinh t/\alpha} - \frac{1}{\sinh t} \right) \frac{1}{\sinh t} - e^{-2t} \right]$$

where also the $O(N^{-2/\alpha})$ corrections are known [46, 52].

Note however that the τ dependence of the formula (44) is not expected to be exact at finite $\tau = Nt$ in the nonequilibrium expansion of the gas, because it assumes the existence of a scaling regime at fixed τ where the two-point function is given by Eq. (42), which is the large- N limit at fixed t . Therefore its validity is not guaranteed in the large- N limit keeping $\tau = Nt$ fixed. However, it is expected to be valid for large values of τ , and to provide the exact asymptotic behavior in the large- τ limit. Thus, assuming a nonsingular matching of the behavior for $\tau \rightarrow \infty$ and $t \rightarrow 0$, it allows us to exactly derive the asymptotic expansion in the small- t limit. Note that

the N and τ dependence in Eq. (44) combines to give a t dependence only. The above considerations imply the following small- t behaviors for the vN and Rényi entanglement entropies of an interval $A = [x_1, x_2]$ ¹

$$S = c_1 [\ln(1/t_\delta) + e_1] - \frac{t_\delta^2}{12} + O(t^4) \quad (47)$$

$$S^{(\alpha)} = c_\alpha [\ln(1/t_\delta) + e_\alpha] \quad (48)$$

$$- \frac{2^{2-2/\alpha} \Gamma[(\alpha+1)/(2\alpha)]^2}{(\alpha-1)\Gamma[(\alpha-1)/(2\alpha)]^2} \cos(2/t_\delta) t_\delta^{2/\alpha} + O(t^{4/\alpha}, t^2)$$

respectively for the vN and Rényi entanglement entropies, where $t_\delta \equiv t/\Delta$. Analogous results can be derived for the particle cumulants, using the large- N ground-state results for homogenous gases without boundaries [27]. We obtain

$$V = \frac{1}{\pi^2} [\ln(1/t_\delta) + w_2] + o(t^0), \quad (49)$$

$$w_2 = 1 + \gamma_E + \ln 2, \quad (50)$$

and for the higher cumulants

$$V^{(2k+1)} = o(t^0) \quad k \geq 1, \quad (51)$$

$$V^{(2k)} = v_{2k} + o(t^0) \quad k \geq 2, \quad (52)$$

where $v_4 = -0.0185104\dots$, $v_6 = 0.00808937\dots$, etc... Note that, in the case of the particle variance, Eq. (49) is in agreement with the asymptotic small- t expansion (40) obtained by the exact large- N expression (39). In Fig. 1 we compare the large- N curves with the above small- t asymptotic expansions.

C. The large-time behavior of entanglement entropies and particle fluctuations

The asymptotic large- t behavior of the observables considered can be derived by replacing the large- t behavior of the one-particle wave functions, cf. Eq. (4),

$$\psi_n(x, t) \approx \sqrt{\frac{2}{\pi^3 t}} \frac{1 - (-1)^n}{n} \quad (53)$$

in the many-body wave function, or in the overlap matrix (20). Note that the above approximations of $\psi_n(x, t)$ are independent of x , corresponding to the fact that when $x \ll v_F t \sim Nt$ the one-particle wave functions within the interval can be approximated by a constant. Thus the overlap matrix reads

$$\mathbb{A}_{nm}(x_1, x_2, t) \approx \frac{2}{\pi^3 t_\delta} \frac{1}{mn} [1 - (-1)^n][1 - (-1)^m], \quad (54)$$

¹ These results can be derived by using the formulas of Ref. [46] for the asymptotic large- N expansion of the entanglement entropies in systems with periodic boundary conditions, by sending $N \rightarrow \infty$, $\ell/L \rightarrow 0$ keeping $N\pi\ell/L = \Delta/t \equiv 1/t_\delta$ fixed.

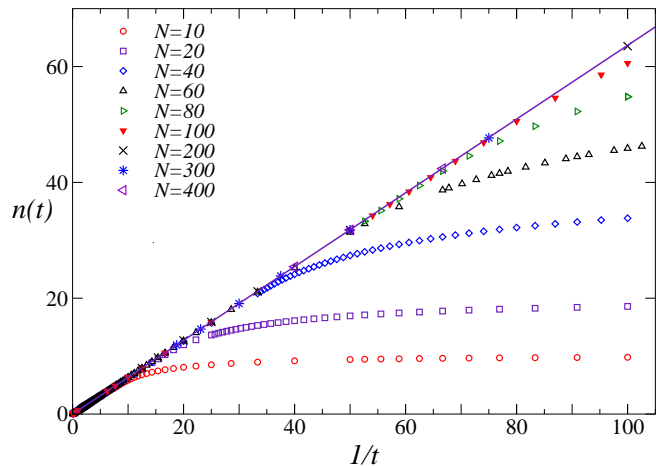


FIG. 2: (Color online) The particle number of the interval $[-1, 1]$. The line shows the large- N limit $n(t) = 2/(\pi t)$, cf. Eq. (35).

where $t_\delta = t/(x_2 - x_1)$. This implies that the large- t regime of the overlap matrix is characterized by only one nonzero eigenvalue a_1 for any N , given by

$$a_1 = \frac{4}{\pi^3 t_\delta} \sum_{k=1}^N \frac{1 - (-1)^k}{k^2} = \frac{1}{\pi t_\delta} [1 + O(N^{-1})] \quad (55)$$

The other eigenvalues get rapidly suppressed in the large- t limit. Numerical results show that

$$\frac{a_2}{a_1} = O(t^{-2}), \quad \frac{a_3}{a_1} = O(t^{-4}), \quad (56)$$

where a_2, a_3 are the next largest eigenvalues.

The largest eigenvalue a_1 determines the asymptotic behaviors of all observables such as the particle number, particle fluctuations and entanglement entropies. We obtain the large- t asymptotic behaviors of the particle cumulants, the Rényi and vN entanglement entropies, respectively

$$V^{(m)} \approx a_1 \approx \frac{1}{\pi t_\delta}, \quad (57)$$

$$S^{(\alpha)} \approx \frac{\alpha}{\alpha-1} a_1 \approx \frac{\alpha}{(\alpha-1)\pi t_\delta}, \quad (58)$$

$$S \approx a_1(1 - \ln a_1) \approx \frac{1}{\pi t_\delta} [\ln t_\delta + 1 + \ln \pi]. \quad (59)$$

D. Numerical results for the interval $[-1, 1]$ at finite N

We want to check the convergence of the particle fluctuations and entanglement entropies to the large- N behaviors derived in the preceding subsections. For this purpose, we compute them at finite particle number N using the method based on the overlap matrix, see Sec. II B. We numerically compute its eigenvalues at fixed

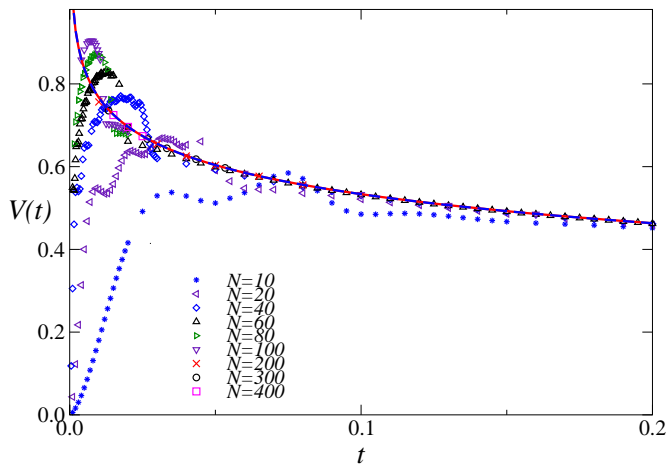


FIG. 3: (Color online) The particle variance of the the interval $[-1, 1]$ for several values of N , compared with the exact (full line) and small- t asymptotic (dashed line) large- N time dependence derived in Sec. III, cf. Eqs. (39) and (49) respectively (which are hardly distinguishable in the figure).

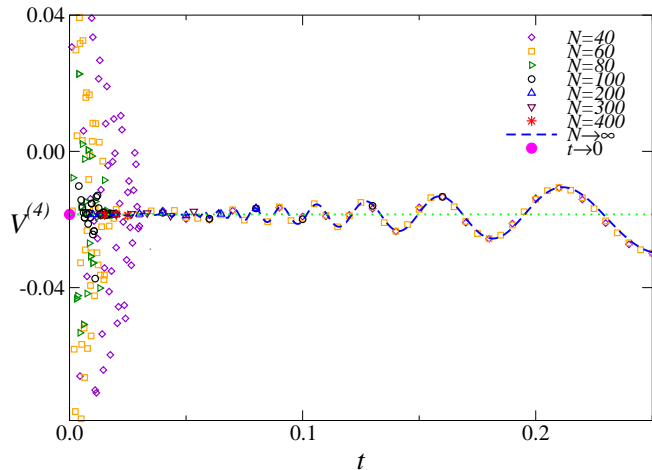


FIG. 4: (Color online) The quartic cumulant for the interval $[-1, 1]$ as a function of the time t , compared with the large- N time dependence derived in Sec. III, and the small- t asymptotic result (52).

t , and then obtain the particle cumulants and the entanglement entropies through Eqs. (22-25). We show results for the interval $A = [-1, 1]$ and several values of N up to $N = 400$. Figs. 2, 3, 4, 5, and 6 show data for the particle number, the second and quartic cumulants, and the vN and $\alpha = 2$ Rényi entanglement entropies. They appear to rapidly converge to the large- N analytical results derived above.

The convergence to the large- N limit keeping fixed t is not uniform when $t \rightarrow 0$. The data at fixed N shown in Figs. 2-6 hint at some nontrivial structures at very small t , which get hidden (pushed toward the $t = 0$ axis) by the large- N limit keeping t fixed.

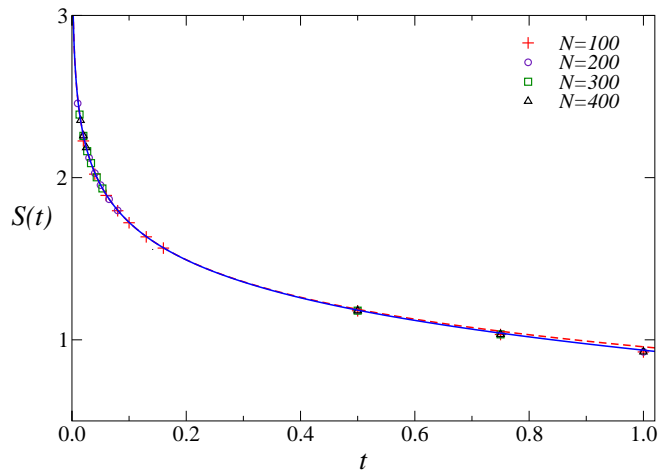


FIG. 5: (Color online) The vN entropy of the interval $[-1, 1]$ as a function of the time t . The dashed lines show the small- t asymptotic behavior $S = c_1[\ln(1/t_\delta) + e_1]$. The full lines show the curves with the next known term, i.e. Eq. (47).

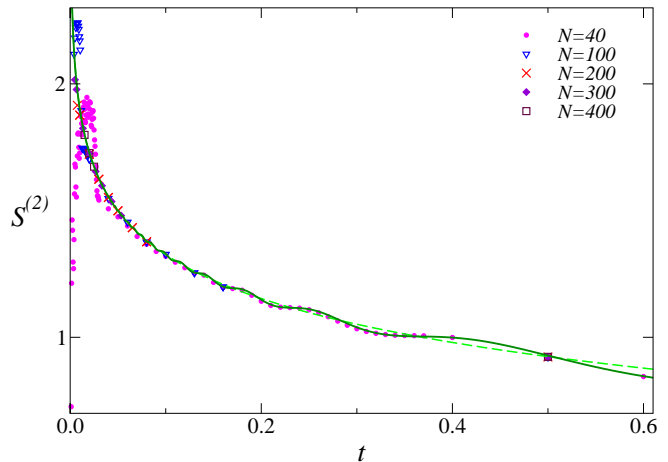


FIG. 6: (Color online) The $\alpha = 2$ Rényi entropy of the interval $[-1, 1]$ as a function of the time t . The dashed lines show the small- t asymptotic behavior $S^{(2)} = c_2[\ln(1/t_\delta) + e_2]$. The full lines show the curves with the next known term, i.e. Eq. (48).

IV. SCALING BEHAVIORS AT SMALL TIME

In order to investigate whether other nontrivial scaling behaviors occur at small times, we consider large- N limits keeping rescaled times $N^\kappa t$ fixed, with $\kappa > 0$. As we shall see, the time evolution of the observables related to extended intervals show other two distinct scaling regimes, with respect to the rescaled time variables

$$\tau \equiv Nt, \quad \theta \equiv N^2 t. \quad (60)$$

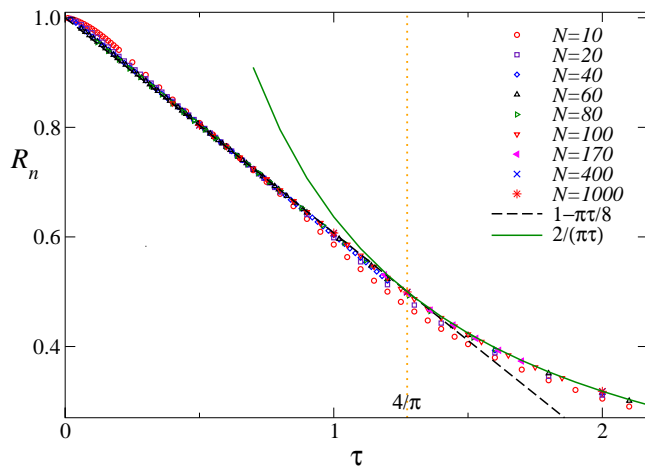


FIG. 7: (Color online) The average particle number of the interval $[-1, 1]$ as a function of $\tau \equiv Nt$. The data appear to converge toward the function (62).

A. Scaling with respect to $\tau \equiv Nt$

We first consider the interval $A = [-1, 1]$, corresponding to the initial trap. In Fig. 7 we show data for the average particle number $n(t)$ versus the scaling variable $\tau = Nt$. The analysis of the data up to $N \approx 10^3$ leads to the time evolution

$$R_n(t) \equiv \frac{n(t)}{N} \approx F_n(\tau), \quad (61)$$

in the large- N limit, where

$$F_n(\tau) = \begin{cases} 1 - \pi\tau/8 & \text{for } \tau \leq 4/\pi, \\ 2/(\pi\tau) & \text{for } \tau \geq 4/\pi \end{cases} \quad (62)$$

Note that the dependence for $\tau \geq 4/\pi$ corresponds to the large- N limit at fixed t , cf. Eq. (35), divided by N . The function $F_n(\tau)$ is approached quite rapidly in the large- N limit, as shown in Fig. 7. We have carefully checked it for some specific values of τ with a precision of $O(10^{-6})$, in both regions $\tau < \pi/4$ and $\tau > \pi/4$ (in particular at $\tau = 1/3, 1/2, 1, 4/\pi, 2$), by extrapolating data up to $N \approx 10^3$ assuming $1/N$ corrections (more precisely, fitting them to $a + b/N + c/N^2$). Note that $F_n(\tau)$ is continuous, but nonanalytic at $\tau = 4/\pi$, where the second derivative is discontinuous. It is worth mentioning that the time $t = 4/(\pi N)$, corresponding to $\tau = 4/\pi$, is the time taken by a particle with speed $k_F = \pi N/2$, which is the Fermi scale of the gas, to cross the interval of size $L = 2$, which is the size of the interval considered.

In Figs. 8 and 9 we show some particle cumulants and entanglement entropies for several values of N up to $N \approx 300$. Their behaviors with increasing N clearly identify two regions, $\tau < 4/\pi$ and $\tau \geq 4/\pi$, related to the two distinct behaviors (62) of the particle-number ratio. For $\tau \geq 4/\pi$ the analysis of the data of the Rényi entanglement entropies show a large- N behavior substantially

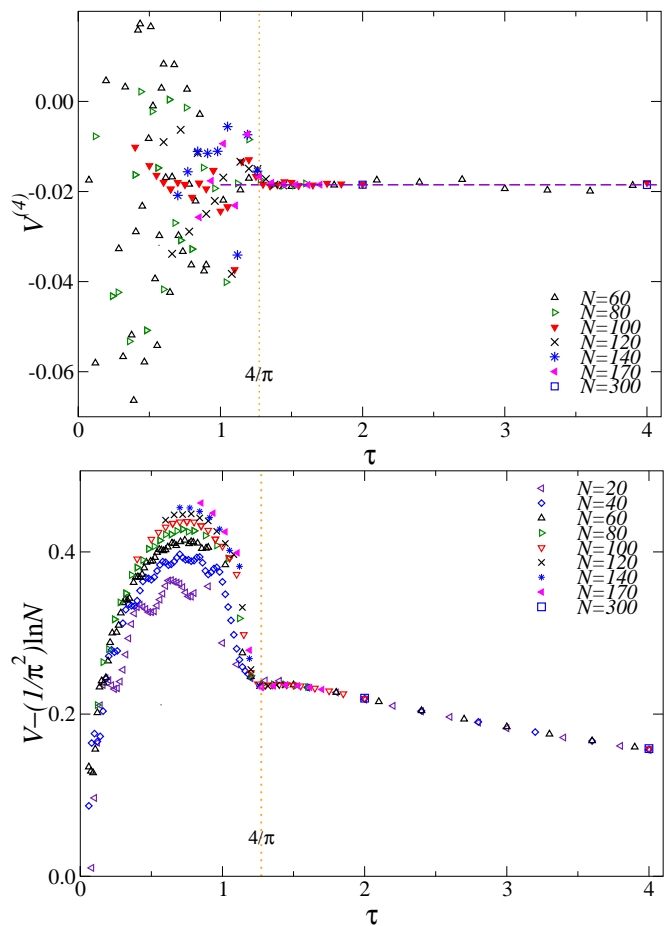


FIG. 8: (Color online) Data for $V - (1/\pi^2) \ln N$ (bottom) and $V^{(4)}$ (top) up to $N = 300$, versus $\tau = Nt$.

consistent with Eq. (44). Indeed,

$$S^{(\alpha)} \approx c_\alpha [\ln N + e_\alpha + F_{S^{(\alpha)}}(\tau)], \quad (63)$$

and, analogously, for the particle cumulants

$$V \approx \frac{1}{\pi^2} [\ln N + w_2 + F_V(\tau)], \quad (64)$$

$$V^{(3)} \approx 0, \quad (65)$$

$$V^{(4)} \approx v_4 = -0.0185104... \quad (66)$$

Moreover, the numerical results are consistent with

$$F_{S^{(\alpha)}}(\tau) = F_V(\tau) = F(\tau), \quad (67)$$

as shown in Fig. 10 by the comparison of the data for $S^{(2)}/c_\alpha - \ln N - e_2$ and $\pi^2 V - \ln N - w_2$ in the region $\tau > 4/\pi$. For sufficiently large τ , $\tau \gtrsim 2$, the large- N limit of the data is well approximated by (see Fig. 9)

$$F(\tau) \approx \ln \sin(2/\tau) \quad (68)$$

which is the τ dependence predicted by the arguments reported in Sec. III B, cf. Eq. (44), for large τ . However, this equation does not appear to be exact, because

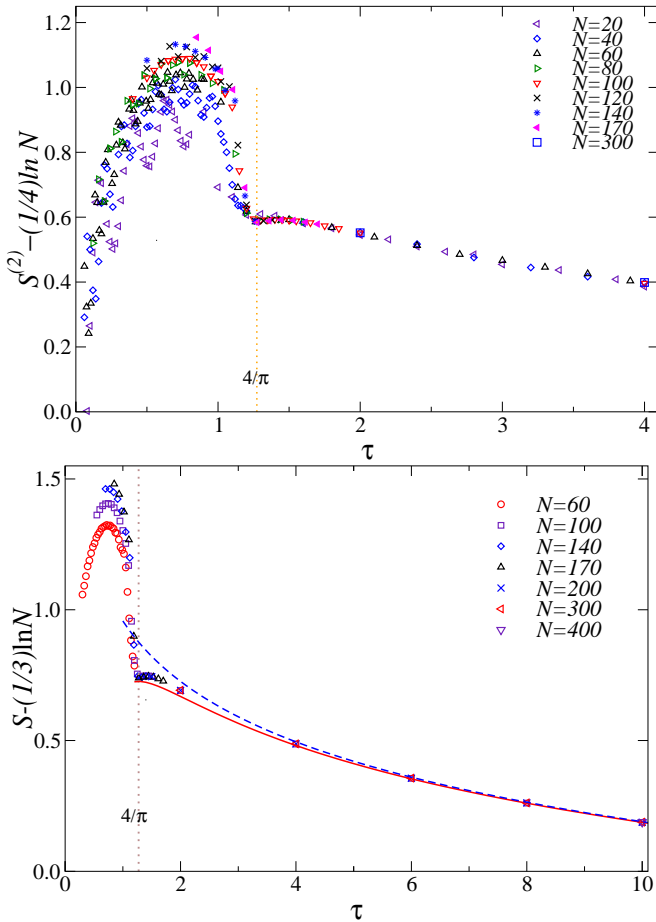


FIG. 9: (Color online) We show subtracted data of the vN and $\alpha = 2$ entropy, respectively $S - (1/3) \ln N$ and $S^{(2)} - (1/4) \ln N$. In the case of the vN entropy we show the curves $(1/3)[\ln(2/\tau) + e_1]$ (dashed line) and $(1/3)[\ln \sin(2/\tau) + e_1]$ (full line) for comparison.

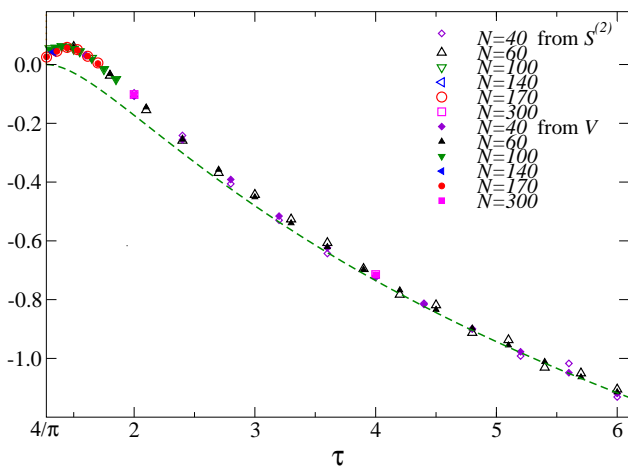


FIG. 10: (Color online) We show $S^{(2)}/c_\alpha - \ln N - e_2$ and $\pi^2 V - \ln N - w_2$ in the region $\tau > 4/\pi$. They suggest the convergence to a unique curve in the large- N limit. The dashed line shows the curve $\ln \sin(2/\tau)$.

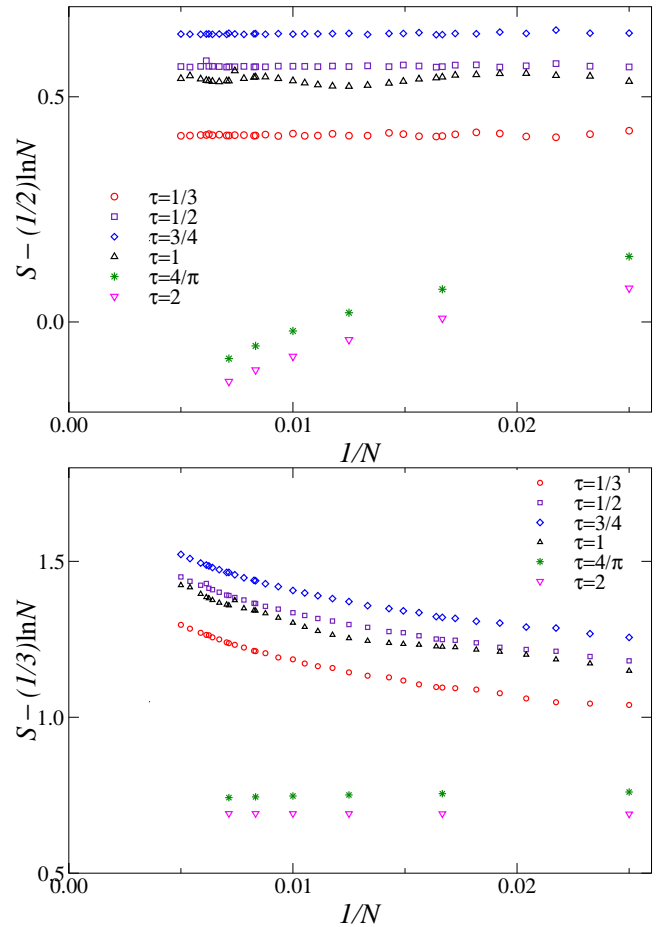


FIG. 11: (Color online) The vN entanglement entropy for some specific values of τ versus $1/N$, after subtracting $(1/3) \ln N$ (bottom) and $(1/2) \ln N$ (top).

there are small $O(\tau^{-2})$ deviations, which increases when approaching the value $\tau = 4/\pi$, see Fig. 10.

The large- N limit is less clear for $\tau < 4/\pi$. The data of the particle variance and entanglement entropies, after subtracting the leading large- N behavior of the initial ground state, does not appear to converge to any large- N curve. The difference is also clearly observed for $V^{(4)}$, see the top Fig. 8, which passes from a stable behavior for $\tau > 4/\pi$ to a behavior characterized by large oscillations. Fig. 11 shows data of S for selected values of τ up to $N = 200$. They show that when we subtract the static leading log behavior, i.e. $(1/3) \ln N$, the data for $\tau > 4/\pi$ look stable, while those for $\tau < 4/\pi$ show a clear trend, see the bottom Fig. 11. On the other hand, the data for $\tau < 4/\pi$ appear much more stable when we subtract $(1/2) \ln N$. This may suggest that a different scaling regime applies in this region, although we cannot exclude that we are just observing a crossover phenomenon with a very slow convergence toward the eventual large- N behavior. This point should deserve further investigation.

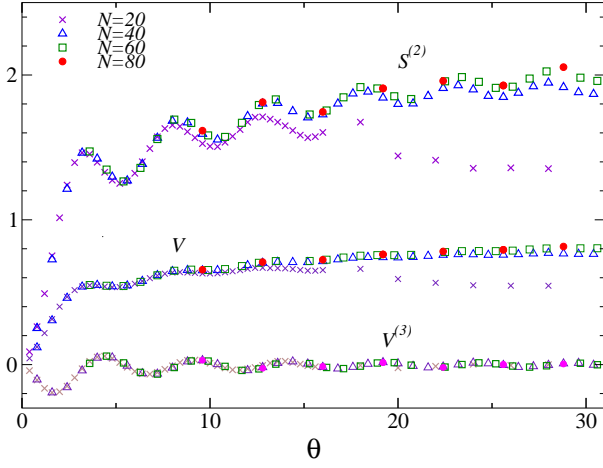


FIG. 12: (Color online) The particle cumulants V and $V^{(3)}$ and the $\alpha = 2$ Rényi entanglement entropy versus $\theta \equiv N^2 t$.

B. Very short-time scaling with respect to $\theta \equiv N^2 t$

Another nontrivial scaling behavior is observed at very small times, in the large- N limit keeping $\theta \equiv N^2 t$ fixed. As shown by Fig. 12, the data provide a clear evidence of the scaling behaviors

$$V^{(m)} \approx w_m(\theta), \quad S^{(\alpha)} \approx \sigma_\alpha(\theta) \quad (69)$$

in the large- N limit keeping θ fixed. Note that the particle-number ratio $R_n \equiv n(t)/N$ is one in this regime, because $1 - R_n(t)$ appears to vanish in the large- N limit keeping θ fixed, with $O(1/N)$ corrections. Therefore, this behavior occurs at very small time scales when even the effective modes at the fermi scale $k_F = \pi N/2$ are still all practically confined within the trap.

C. Particle cumulants and entanglement entropies of the interval $[-1/2, 1/2]$.

We now discuss the behavior of the particle cumulants and entanglement entropies of an interval corresponding to a half of the initial trap, i.e. $[-l/2, l/2] \equiv [-1/2, 1/2]$. The average particle number within this interval at $t = 0$ is

$$\begin{aligned} n(0) &= \frac{N}{2} + \int_{-1/2}^{1/2} dx \left[\frac{1}{4} - \frac{\sin[\pi(N+1/2)(1+x)]}{4 \sin[\pi(1+x)/2]} \right] \\ &= \frac{N}{2} \left[1 + \frac{1}{2N} + O(N^{-2}) \right]. \end{aligned} \quad (70)$$

The particle cumulants are given by [27]

$$V^{(2)}(0) = \frac{1}{\pi^2} (\ln N + w_2) + O(N^{-1}), \quad (71)$$

$$V^{(2k+1)}(0) = o(N^0), \quad (72)$$

$$V^{(2k)}(0) = v_{2k} + o(N^0), \quad k > 2, \quad (73)$$

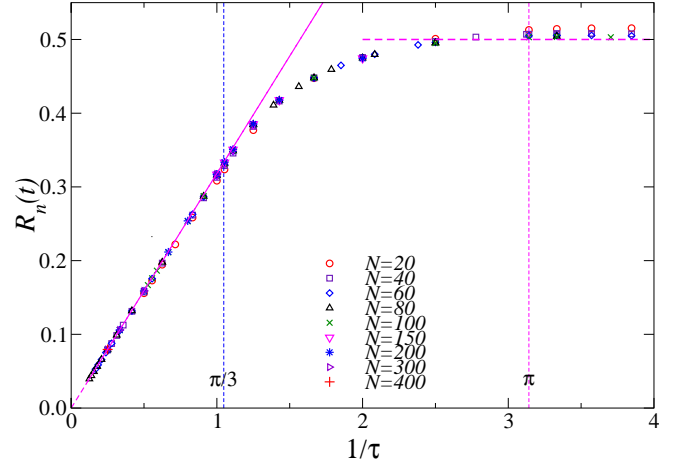


FIG. 13: (Color online) Particle number for the interval $[-1/2, 1/2]$. The dashed lines show the small- τ and large- τ behaviors of Eq. (76).

and the Rényi entanglement entropies [45]

$$S^{(\alpha)}(0) = c_\alpha (\ln N + e_\alpha) + O(N^{-1/\alpha}) \quad (74)$$

where the constants w_2 , v_{2k} , e_α have already been defined in Eqs (46), (50) and (52).

The large- N behavior at fixed t has been already determined in Sec. III. Here, we focus on the large- N behavior at fixed $\tau \equiv Nt$, to check how it depends on the interval considered.

The ratio between the particle number $n(t)$ within the interval and the total particle N rapidly approach a large- N scaling function of $\tau \equiv Nt$, as shown by the data up to $N \approx 200$ of Fig. 13. Therefore,

$$R_n(t) \equiv \frac{n(t)}{N} \approx F_n(\tau), \quad (75)$$

Moreover, the data provide a strong evidence of simple behaviors in the regions $\tau < 1/\pi$ and $\tau > 3/\pi$, i.e.

$$F_n(\tau) = \begin{cases} 1/2 & \text{for } \tau \leq 1/\pi, \\ 1/(\pi\tau) & \text{for } \tau \geq 3/\pi \end{cases} \quad (76)$$

Again, the large- τ behavior corresponds to the large- N time dependence $n(t) = 1/(\pi t)$.

Concerning the other observables, again the data show the presence of different large- N regimes. In Fig. 14 we show the vN entanglement entropy after subtracting the corresponding $t = 0$ asymptotic formula (74). For $\tau \gtrsim 3/\pi$ the data provides a strong evidence of large- N behaviors analogous to those of Eqs. (63-66). Also Eq. (68) turns out to be valid, with

$$F(\tau) \approx \ln \sin(1/\tau) \quad (77)$$

but again this result does not appear exact, showing increasing, but always very small, deviations when approaching $\tau = 3/\pi$. An analogous scaling, as in Eqs. (63-66), is found for $\tau < 1/\pi$. On the other hand, we have

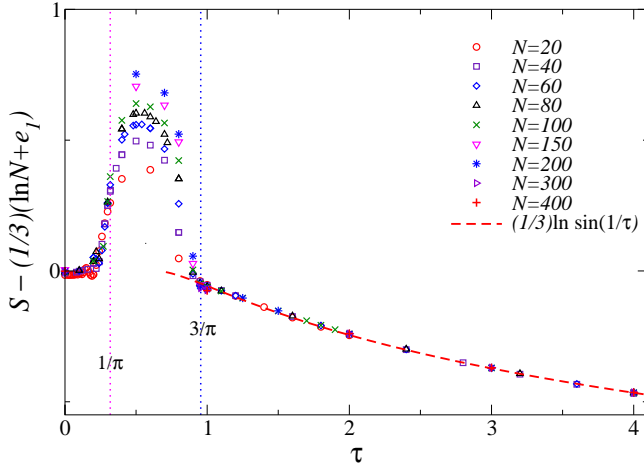


FIG. 14: (Color online) We report data for the vN entanglement entropy after subtraction of the asymptotic large- N $t = 0$ expansion $(1/3)(\ln N + e_1)$. The dashed line shows the function $(1/3) \ln \sin(1/\tau)$.

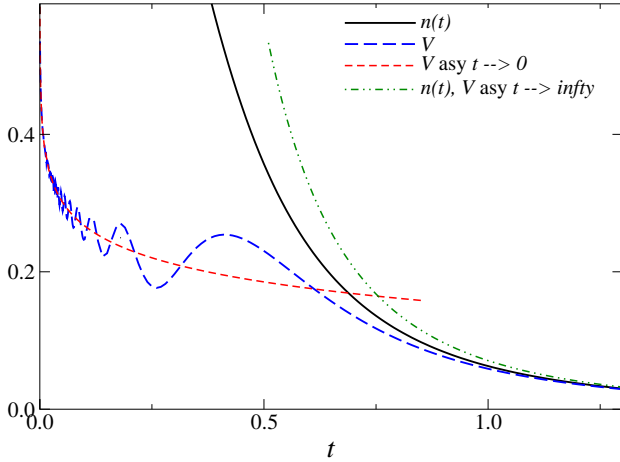


FIG. 15: (Color online) The large- N time dependence of the particle cumulants, and, for comparison, their small- t asymptotic behavior, for the interval $[0, 1]$ when only one wall is dropped and the gas expands along the positive real axis.

again an intermediate region, for $1/\pi \lesssim \tau \lesssim 3/\pi$ where the data appear to favor a different $\ln N$ behavior at large- N , with $S \approx (1/2) \ln N$ instead of $(1/3) \ln N$.

V. TIME EVOLUTION IN THE CASE ONLY ONE WALL DROPS

We now consider the case only one wall is instantaneously dropped and the gas expands along the positive axis, which is described by the many-body wave function reported in Sec. II A 2. We proceed as in Sec. III A. The large- N two-point function (taken at fixed t) can be again derived using the completeness relation, cf. Eq. (30), ob-

taining

$$\mathbb{C}_A(x, y, t) = \frac{\sin[(y-x)/t]}{\pi(y-x)} - \frac{\sin[(y+x)/t]}{\pi(y+x)}, \quad (78)$$

after dropping an irrelevant phase. In the case of an interval $A = [0, x]$, the particle number reads

$$n(t) = \text{Tr } \mathbb{C}_A = \frac{1}{\pi t_\delta} - \frac{\text{Si}(2/t_\delta)}{\pi}, \quad (79)$$

where

$$t_\delta = t/x \quad (80)$$

Results for the large- N limit of the other observables can be obtained by replacing $\mathbb{C}_A(x, y, t)$ in the expansion of Eq. (18). Fig. 15 shows the large- N limit of the particle number, and the particle variance for the interval $[0, 1]$, corresponding to the initial trap.

In order to compute the entanglement entropies, we note that the large- N two-point function (78) appears as the continuum limit of the two-point function of free lattice fermions at equilibrium in the thermodynamic limit with open boundary conditions, see Ref. [53]. Exploiting again this correspondence, as in Sec. III A, we derive the small- t asymptotic behaviors of the entanglement entropies of the interval $A = [0, x]$ extracting the appropriate continuum limit from known asymptotic results for free fermions with open boundary conditions [46, 53], obtaining²

$$S^{(\alpha)} = \frac{c_\alpha}{2} [\ln(1/t_\delta) + e_\alpha + \ln 2] + \frac{2^{1-2/\alpha} \Gamma[(\alpha+1)/(2\alpha)]}{(\alpha-1) \Gamma[(\alpha-1)/(2\alpha)]} \sin(1/t_\delta) t_\delta^{1/\alpha} + O(t^{2/\alpha}) \quad (81)$$

Analogously, we can derive the asymptotic small- t behavior of the particle cumulants using the results of Ref. [27],

$$V \approx \frac{1}{2\pi^2} [\ln(1/t_\delta) + w_2 + \ln 2], \quad (82)$$

$$V^{(3)} \approx 0, \quad (83)$$

$$V^{(4)} = v_4/2, \quad (84)$$

etc....

The large- t behavior can be determined as in Sec. III C, by replacing the large- t approximation of the one-particle wave functions in the overlap matrix (20), i.e.

$$\phi_n(x, t) \approx \frac{2(-1)^n x}{n\sqrt{\pi^3 t^3}}. \quad (85)$$

² These results can be derived by using the formulas of Ref. [46] for the asymptotic large- N expansion of the entanglement entropies in systems with open boundary conditions, by sending $N \rightarrow \infty$, $\ell/L \rightarrow 0$ keeping $N\pi\ell/L = \Delta/t \equiv 1/t_\delta$ fixed.

Thus, the overlap matrix of the interval $A = [0, x]$ is

$$\mathbb{A}_{nm}(t) \approx \frac{4x^3}{3\pi^3 t^3} \frac{(-1)^n}{n} \frac{(-1)^m}{m}. \quad (86)$$

Again, this form of the overlap matrix has only one nonzero eigenvalue

$$a_1 = \frac{4x^3}{3\pi^3 t^3} \sum_{n=1}^N \frac{1}{n^2} = \frac{2x^3}{9\pi^3 t^3} [1 + O(1/N)] \quad (87)$$

We thus obtain the large- t behaviors

$$n(t) \approx a_1 \approx \frac{2}{9\pi^3 t_\delta^3}, \quad (88)$$

$$V^{(i)} \approx a_1 \approx \frac{2}{9\pi^3 t_\delta^3}, \quad (89)$$

$$S^{(\alpha)} \approx \frac{\alpha}{\alpha-1} a_1 \approx \frac{\alpha}{(\alpha-1) 9\pi^3 t_\delta^3}, \quad (90)$$

$$S \approx a_1 (1 - \ln a_1) \approx \frac{2}{3\pi^3 t_\delta^3} \ln t_\delta + \dots \quad (91)$$

It is interesting to compare these results with those of the gas which freely expands along both directions, cf. Eqs. (35) and (57-59). They show different power laws, in particular, we note the fact that, at large times, the trap gets emptied much faster when only one wall drops.

VI. FERMION GASES IN TIME-DEPENDENT HARMONIC TRAPS

In this section we study the nonequilibrium evolution of fermion gases in a time-dependent confining harmonic potential,

$$V(x, t) = \frac{1}{2} \kappa(t) x^2, \quad (92)$$

starting from an equilibrium ground state configuration with initial trap size

$$l_0 = \kappa_0^{-1/2}. \quad (93)$$

Particular interesting cases are the instantaneous change to a confining potential with different trap size l_f , i.e. $\kappa(t) = \kappa_f$ for $t > 0$, or the complete drop of the trap, $\kappa(t) = 0$ for $t > 0$.

A. The time-dependent many-body wave function

The time-dependent wave function Ψ of N free spinless fermions, with $\Psi(x, 0)$ given by the ground state of the Hamiltonian at $t = 0$, can be written as [54, 55]

$$\Psi(x_1, \dots, x_N; t) = \frac{1}{\sqrt{N!}} \det[\psi_i(x_j, t)],$$

where the determinant involves the one-particle wave functions $\psi_j(x, t)$ associated with the N lowest eigensolutions of the Hamiltonian at $t = 0$. They are the solutions $\psi_j(x, t)$ of the one-particle Schrödinger equation

$$i \frac{\partial \psi_j(x, t)}{\partial t} = \left[-\frac{1}{2} \partial_x^2 + V(x, t) \right] \psi_j(x, t), \quad (94)$$

with the initial condition $\psi_j(x, 0) = \phi_j(x)$ where $\phi_j(x)$ are the eigensolutions of the Hamiltonian at $t = 0$, characterized by a trap size l_0 , with eigenvalue $E_j = (j + 1/2)/l_0$. The solution can be expressed introducing a time-dependent function $s(t)$, writing [54, 56]

$$\psi_j(x, t) = s^{-1/2} \phi_j(\tilde{x}) \exp \left(i \frac{1}{2} \dot{s} s \tilde{x}^2 - i E_j \int_0^t s^{-2} dt' \right), \quad (95)$$

where

$$\tilde{x} \equiv x/s, \quad (96)$$

$\phi_j(x)$ is the j^{th} eigenfunction of the Schrödinger equation of the one-particle Hamiltonian at $t = 0$, thus with trap size l_0 , and the real function $s(t)$ satisfies the nonlinear differential equation

$$\ddot{s} + \kappa(t)s = \kappa_0 s^{-3} \quad (97)$$

with initial conditions $s(0) = 1$ and $\dot{s}(0) = 0$. In App. A we report some explicit solutions of the above equation, for an instantaneous drop of the trap, an instantaneous change to a trap of different size, in the case of a linear time dependence of the trapping potential, and a drop of the trap driven by a linear time dependence.

The above results allow us to relate the time-dependent nonequilibrium many-body function for $t > 0$ to the equilibrium many-body wave function at $t = 0$, writing [8]

$$\Psi(x_1, \dots, x_N; t) = s^{-N/2} \Psi(\tilde{x}_1, \dots, \tilde{x}_N; 0) \times \exp \left(i \frac{1}{2} \dot{s} s \sum_j \tilde{x}_j^2 - i \sum_j E_j \int_0^t s^{-2} dt' \right), \quad (98)$$

where $\Psi(x_1, \dots, x_N; 0)$ is the wave function of the ground state of the Hamiltonian at $t = 0$.

B. Self-similar time evolution of density correlations and spatial entanglement

1. Time dependence of the particle correlations

The equal-time two-point function can be derived using Eq. (98),

$$C(x, y, t) = \sum_{i=1}^N \psi_i(x, t)^* \psi_i(y, t) = \sum_{i=1}^N \hat{\psi}_i(x, t)^* \hat{\psi}_i(y, t), \quad (99)$$

where

$$\hat{\psi}_j(x, t) = s^{-1/2} \phi_j(\tilde{x}) \exp\left(i \frac{1}{2} \dot{s} s \tilde{x}^2\right). \quad (100)$$

This implies that

$$C(x, y; t) = s^{-1} C(\tilde{x}, \tilde{y}; 0) \exp\left[i \frac{1}{2} \dot{s} s (\tilde{y}^2 - \tilde{x}^2)\right], \quad (101)$$

where $C(x, y; 0)$ is the equilibrium correlation function for the trap size $l = l_0$, i.e. $C(x, y; 0) = C(x, y)|_{l=l_0}$.

Eq. (101) implies that the one-body entanglement entropy remains unchanged during the time evolution. At equilibrium, the one-particle Rényi entanglement entropies $\sigma^{(\alpha)}$ of the ground state of trapped free fermion gases increase logarithmically, indeed

$$\sigma^{(\alpha)} \equiv \frac{1}{1-\alpha} \ln \text{Tr} \rho_1(x, y)^\alpha = \ln N \quad (102)$$

where $\rho_1(x, y) = C(x, y)/N$ is the one-particle density matrix. The one-particle Rényi entropies do not change during the time evolution, because the time-dependent one-particle density matrix $\rho_1(x, y, t) = C(x, y, t)/N$ satisfies

$$\text{Tr} \rho_1(x, y; t)^\alpha = \text{Tr} \rho_1(x, y; 0)^\alpha. \quad (103)$$

The particle density $\rho(x, t)$ and the current $j(x, t)$, which enters the conservation law

$$\partial_t \rho(x; t) + \partial_x j(x; t) = 0, \quad (104)$$

show the simple behaviors

$$\rho(x; t) = C(x, x, t) = \frac{1}{s} \rho(\tilde{x}; 0), \quad (105)$$

$$j(x; t) = -\frac{i}{2} \sum_{i=1}^N [\psi_i(x, t)^* \partial_x \psi_i(x, t) - \partial_x \psi_i(x, t)^* \psi_i(x, t)] = \frac{\dot{s}}{s} \tilde{x} \rho(\tilde{x}; 0) \quad (106)$$

where $\rho(\tilde{x}; 0) = \rho_s(x)$ is the static particle density for the initial trap size l_0 .

The ground-state (equilibrium) particle density for a large number of particles is given by (setting $l_0 = 1$) [57, 58]

$$\rho_s(x) = N^{1/2} [R_\rho(\zeta) + O(1/N)], \quad (107)$$

where $\zeta \equiv x/N^{1/2}$, and

$$R_\rho(\zeta) = \frac{1}{\pi} \sqrt{2 - \zeta^2}, \quad \zeta \leq \zeta_c = \sqrt{2}, \quad (108)$$

and $R_\rho(\zeta) = 0$ for $\zeta > \zeta_c = \sqrt{2}$. By integrating the particle density, we obtain the average particle number over extended intervals. For example, by integrating Eq. (107)

over the symmetric interval $Z = [-x, x]$ around the center of the trap, we obtain

$$\frac{N_Z(x)}{N} = p(\zeta) + O(1/N), \quad \zeta \equiv x/N^{1/2}, \quad (109)$$

$$p(\zeta) = \frac{1}{\pi} \left[\zeta \sqrt{2 - \zeta^2} + 2 \arcsin(\zeta/\sqrt{2}) \right] \quad (110)$$

Therefore, using Eq. (105), we obtain that the large- N time dependence of the average particle number with $S = [-x, x]$ is given by

$$\frac{N_Z(x, t)}{N} \approx p[\zeta/s(t)] \quad (111)$$

The equal-time density-density correlation behaves as

$$G_n(x, y; t) = s^{-2} G_n(\tilde{x}, \tilde{y}; 0) \quad (112)$$

where $G_n(\tilde{x}, \tilde{y}; 0)$ is the static particle density correlation for the initial trap size. The large- N scaling of its space dependence differs significantly from that of the particle density, indeed its large- N behavior is [59]

$$G_n(x, y) \approx N R_G(N^{1/2}x, N^{1/2}y), \quad (113)$$

for $x \neq y$.

A discussion of the adiabatic approximation of the unitary evolution for slow changes of the harmonic potential, and its limitations, can be found in Ref. [59].

2. Particle cumulants and entanglement entropies

The time evolution of the bipartite entanglement entropy $S^{(\alpha)}(x_1, x_2; t)$ and the particle cumulants $V^{(m)}(x_1, x_2; t)$ of an interval $[x_1, x_2]$ can be computed using the method based on the overlap matrix, outlined in Sec. II B. The time-dependent overlap matrix reads

$$A_{ij}(x_1, x_2; t) = \int_{x_1}^{x_2} dz \hat{\psi}_i(z, t)^* \hat{\psi}_j(z, t) = A_{ij}(\tilde{x}_1, \tilde{x}_2; 0), \quad (114)$$

where $A_{ij}(\tilde{x}_1, \tilde{x}_2; 0)$ is the static matrix of the interval $[\tilde{x}_1, \tilde{x}_2]$ for the initial trap size. This implies that, in the presence of time-dependent harmonic potential, the entanglement entropies and particle cumulants of extended subsystems behave as

$$S^{(\alpha)}(x_1, x_2; t) = S^{(\alpha)}(\tilde{x}_1, \tilde{x}_2; 0), \quad (115)$$

$$V^{(m)}(x_1, x_2; t) = V^{(m)}(\tilde{x}_1, \tilde{x}_2; 0). \quad (116)$$

This time dependence shows the remarkable property that their evolution in a time-dependent harmonic potential simply corresponds to a global rescaling of the space dependence within the ground state of the initial Hamiltonian for a trap size l_0 .

We know some asymptotic large- N behaviors of the ground-state entanglement properties of Fermi gas in the presence of an external harmonic potential [40]. Setting

$l_0 = 1$, the asymptotic large- N expansion of the half-space (i.e. of the infinite interval $[-\infty, 0]$ where $x = 0$ is the center of the trap) entanglement entropies is [40]

$$S_{\text{HS}}^{(\alpha)} = \frac{c_\alpha}{2} \left[\ln N + \ln 4 + e_\alpha + O(N^{-1/\alpha}) \right], \quad (117)$$

where c_α and e_α are the constants reported in Eqs. (45) and (46). For the half-space particle cumulants we have

$$V_{\text{HS}} = \frac{1}{2\pi^2} \left[\ln N + \ln 4 + w_2 + O(N^{-1}) \right], \quad (118)$$

$$V_{\text{HS}}^{(2i+1)} = o(N^0) \quad \text{for } i > 2, \quad (119)$$

$$V_{\text{HS}}^{(2i)} = \frac{v_{2i}}{2} + o(N^0) \quad \text{for } i > 2, \quad (120)$$

where w_2 and v_{2i} are the constants appearing in the Eqs. (50-52). Note that the half-space particle cumulants and entanglement entropies remain constant during the time evolution. Moreover, in any free expansion from the harmonic trap, the entanglement of any semi-infinite piece $[-\infty, x]$ tends asymptotically to $S_{\text{HS}}^{(\alpha)}$.

The entanglement entropies and the particle variance of the symmetric interval $Z = [-x, x]$ around the center of trap behave as

$$S_Z^{(\alpha)}(x) \approx c_\alpha \left[\ln N + e_\alpha + \ln 2 + f_{S^{(\alpha)}}(\zeta) \right], \quad (121)$$

$$V_Z(x) \approx \frac{1}{\pi^2} \left[\ln N + w_2 + \ln 2 + f_V(\zeta) \right], \quad (122)$$

where $\zeta = x/N^{1/2}$. Moreover, the large- N extrapolation of numerical (practically exact) results at fixed N turns out to be well described by the function [40]

$$f_{S^{(\alpha)}}(\zeta) = f_V(\zeta) = \ln \sin(\pi\zeta/\sqrt{2}) + \ln(4/\pi) \quad (123)$$

The higher cumulants have a much simpler large- N behavior, i.e. $V_Z^{(2k+1)} \approx 0$ and $V_Z^{(2k)} \approx v_{2k}/2$. The time dependence of these quantities during the expansion of the gas can be obtained by rescaling the space dependence of these formulas according to Eqs. (115) and (116).

Finally, we mention that analogous results, such as Eqs. (105), (112), (115) and (117-122), apply also to a 1D gas of impenetrable bosons in time-dependent harmonic traps. Moreover, these results can be straightforwardly extended to higher-dimensional trapped systems. One can easily show that the evolution of the entanglement entropy of connected bipartitions in a harmonic potential corresponds to a global rescaling of the multidimensional space.

C. Large- t behavior in the case of an infinite expansion

In the case on an infinite expansion of the gas, due to the drop of the trap, $s(t)$ diverges for $t \rightarrow \infty$. The results of the previous section imply that the entanglement entropies of any finite interval vanish in the long time limit.

On the other hand, the entanglement entropies and particle cumulants of any semi-infinite piece $[-\infty, x]$ tends asymptotically to $S^{(\alpha)}(-\infty, 0; 0)$ and $V^{(m)}(-\infty, 0; 0)$, given by Eqs. (121) and (122) respectively.

The large- t behavior of the entanglement entropies and particle cumulants of the symmetric interval $Z = [-x, x]$ can be analytically inferred by observing that, since the time evolution is characterized by a time-dependent spatial rescaling $x \rightarrow x/s(t)$, large time implies $x/s(t) \rightarrow 0$. Thus we should evaluate the overlap matrix for a small interval around the center

$$A_{nm} = \int_{-x}^x dx \phi_n(x) \phi_m(x) \approx 2x \phi_n(0) \phi_m(0), \quad (124)$$

which has only one nonzero eigenvalue

$$a_1 = 2x \sum_{i=1}^N \phi_i(0)^2 = 2x \rho(N; 0) \quad (125)$$

with

$$\rho(N; 0) = \sum_{i=1}^N \frac{\pi^{1/2} 2^{i-1}}{(i-1)! \Gamma(1-i/2)^2} = \quad (126)$$

$$= N^{1/2} \frac{\sqrt{2}}{\pi} \left[1 + \frac{(-1)^N}{4N} + O(N^{-2}) \right] \quad (127)$$

Exact calculations at fixed N and t show that

$$\frac{a_2}{a_1} = O(x^2) \quad (128)$$

where a_2 is the next largest eigenvalue. Thus, the large- t evolution is determined by only one eigenvalue

$$a_1(t) = \frac{2x}{s(t)} \rho(N; 0) \quad \text{for } s(t) \rightarrow \infty, \quad (129)$$

which determines the large- t behaviors of the observables which can be derived from the eigenvalues of the overlap matrix, such as the average particle number, the particle cumulants and the entanglement entropies, as shown in Sec. III C.

D. Free expansion after the drop of the trap

In this section we consider the case of a quantum quench after an instantaneous removal of the harmonic trap starting from the ground state of a harmonic potential of frequency $\sqrt{\kappa_0}$, for which we have the analytic solution

$$s(t) = \sqrt{1+t^2} \quad (130)$$

where we set $\kappa_0 = l_0^{-2} = 1$. The time dependence of the observables considered in this paper can be easily found for other time dependences of the trap size, such as those whose scaling functions $s(t)$ are reported in App. A, by essentially the same steps as below.

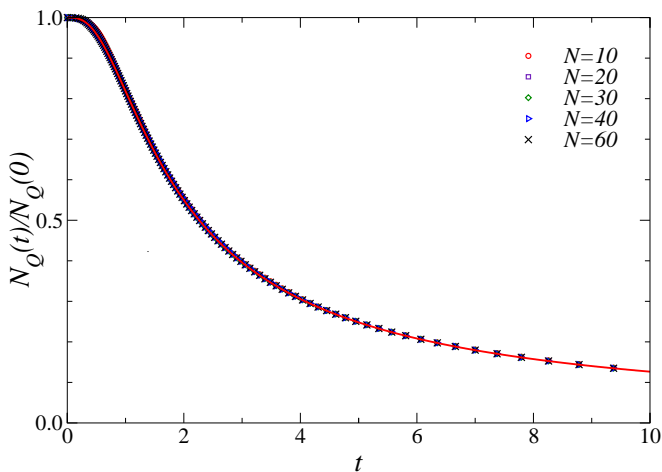


FIG. 16: (Color online) The average particle number of an interval $Q = [-b, b]$ with $b = \sqrt{2}N^{1/2}$. The full line shows the large- N limit (134).

We consider the large- N limit associated with the N -dependent interval

$$Q = [-b(N), b(N)], \quad b(N) = \sqrt{2}N^{1/2}, \quad (131)$$

around the center of the trap, so that all particles are initially contained within Q , at least asymptotically in the large- N limit. Indeed, the initial average number of particles within Q is given by

$$\frac{N_Q(0)}{N} = 1 - \frac{c}{N} + \dots \quad (132)$$

where ³

$$c = 2 \int_0^\infty \left[2^{1/2} |\text{Ai}'(2^{1/2}z)|^2 - 2z |\text{Ai}(2^{1/2}z)|^2 \right] dz \quad (133)$$

which gives $c = 0.0612588\dots$

In the large- N limit, the time dependence of the average particle number within Q is obtained from Eq. (111),

$$\frac{N_Q(t)}{N} \approx \frac{N_Q(t)}{N_Q(0)} \approx p[\sqrt{2}/s(t)], \quad (134)$$

which behaves as $4/(\pi t)$ for large t . Fig. 16 reports results obtained at finite N up to $N = 60$, which show that the convergence to the large- N limit is quite rapid.

The time dependence of the particle cumulants and entanglement entropies can be derived from the corresponding static space dependence, cf. Eqs. (121-123), by replacing ζ with $\sqrt{2}/s(t)$. In particular, the vN entropy is expected to behave as

$$S_Q(t) = \frac{1}{3} [\ln N + e_1 + \ln 2 + f_Q(\pi/s(t))], \quad (135)$$

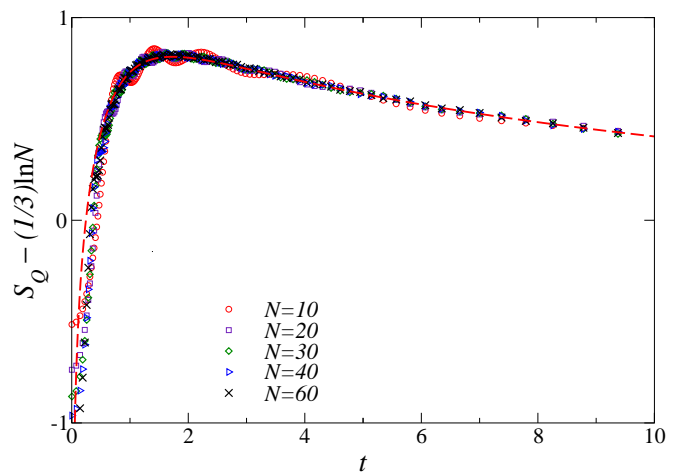


FIG. 17: (Color online) The vN entanglement entropy of the interval Q . The dashed line shows the function given by Eqs. (135) and (136).

with

$$f_Q(x) \approx \ln \sin x + \ln(2/\pi). \quad (136)$$

Fig. 17 shows the vN entanglement entropy of the interval A up to $N = 60$, which appear to rapidly approach the above large- N time dependence (the convergence appears slower at small times).

The large-time behavior is characterized by another scaling behavior, with respect to the time variable

$$t_l \equiv t/N. \quad (137)$$

This is already suggested by the analysis of Sec. VI C. Indeed, Eq. (129) gives

$$a_1(t) \approx \frac{4}{\pi} \frac{N}{t} = \frac{4}{\pi t_l} \quad (138)$$

for the largest eigenvalue of the overlap matrix of the interval Q . The analysis of the numerical data at finite N supports it, see, e.g., the vN entanglement entropy versus t_l shown in Fig. 18. The small- t_l behavior is obtained by matching it with the large- t behavior given by Eq. (135), i.e.

$$S_Q \approx \frac{1}{3} [\ln(1/t_l) + e_1 + \ln 4] \quad (139)$$

The large- t_l behavior is obtained using Eq. (138),

$$S_Q \approx \frac{4}{\pi t_l} [\ln t_l + 1 - \ln(4/\pi)] \quad (140)$$

Analogous results can be derived for the Rényi entropies and the particle cumulants.

VII. CONCLUSIONS

We study the nonequilibrium dynamics of a 1D non-interacting spinless Fermi gas which is initially confined

³ The derivation of Eqs. (132) and (133) uses results of Refs. [40, 59] for the *anomalous* power-law large- N scaling behavior at the effective boundaries of the harmonic trap.

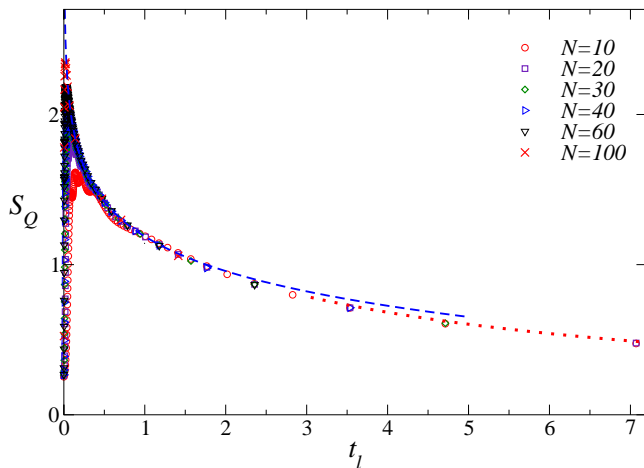


FIG. 18: (Color online) Large-time scaling of the vN entanglement entropy of the interval A with respect to $t_l \equiv t/N$. The dashed and dotted lines show the asymptotic behaviors (139) and (140) respectively.

within a limited region of space (trap) by an external force, and then released from the trap. As initial condition at $t = 0$, we consider a Fermi gas of N particles in the ground state within hard walls or in the presence of an external harmonic potential, as in most experimental realizations of cold atom systems. We study the behavior of the quantum correlations related to extended spatial regions, such as the entanglement entropy and the particle fluctuations, after the instantaneous drop of the trap, or during a change of the harmonic potential.

In order to investigate the entanglement properties during the expansion, we consider quantum correlations associated with extended regions of space in proximity to the initial trap, such as the vN and Rényi entanglement entropies, and the particle cumulants which characterize the distribution of the particle number within the space region. In order to also investigate the differences related to the particular quenching procedure and/or the initial conditions, we consider Fermi gases of N particles initially trapped by hard walls, which freely expand after one or both walls drop instantaneously, and by a harmonic potential, which gives rise to a nonhomogenous initial ground state due to the space-dependence of the confining potential. In all cases, we focus on the behavior in the limit of a large number of particles. Different dynamics regimes are found during the time evolution, which are distinguished by focusing on the large- N limit keeping t fixed or keeping t times appropriate powers of N fixed.

In the following we summarize the main results achieved by this study.

In the case of the free expansion of a 1D Fermi gas released from hard-wall traps located within the interval $[-l, l]$ (we set $l = 1$ without losing generality), we find that in large- N limit the equal-time two-point function assumes a relatively simple form, given by Eq. (33).

It turns out to be an appropriate continuum limit of the two-point function of a lattice free-fermion model without boundaries at equilibrium in the thermodynamic limit. This allows us to infer exact small-time asymptotic behaviors in the large- N limit from corresponding asymptotic expansions of bipartite entanglement entropies in homogeneous systems, already obtained by conformal-field theory and other exact methods [44, 51–53]. In particular, for an extended interval $[x_1, x_2]$ the small- t behavior of the $\alpha = 1$ vN and Rényi entanglement entropies of an interval are given by

$$S^{(\alpha)} = c_\alpha [\ln(1/t_\delta) + e_\alpha] + O(t^{2/\alpha}), \quad (141)$$

$$c_\alpha = \frac{1 + \alpha^{-1}}{6}, \quad t_\delta \equiv t/(x_2 - x_1), \quad (142)$$

where the constant e_α is given by Eq. (46), and also the $O(t^{2/\alpha})$ corrections are computed, cf. Eqs. (47) and (48). Note that the leading logarithmic term corresponds to the leading logarithmic term of the Rényi entanglement entropy of an interval of length ℓ

$$S^{(\alpha)} \approx c_\alpha \ln \ell + b_\alpha \quad (143)$$

which is the universal behavior predicted by the conformal field theory and determined by the corresponding central charge $c = 1$ [12, 51]. Analogous results are also obtained for the particle cumulants, in particular the particle variance behaves as

$$V = \frac{1}{\pi^2} [\ln(1/t_\delta) + w_2 + O(t^2)], \quad (144)$$

see Eqs. (38), (39) and (49) for more details. Moreover, higher cumulants behave as $V^{(2k+1)} = o(t^0)$ (odd cumulants) and $V^{(2k)} = v_{2k} + o(t^0)$ for $k \geq 2$, cf. Eq. (52). The large- t behaviors are also computed, and are characterized by negative powers laws, see Sec. III C. In particular, the large-time behavior of the vN entropy is

$$S \approx \frac{1}{\pi t_\delta} [\ln t_\delta + 1 + \ln \pi] \quad (145)$$

Concerning the above results a few further comments are in order.

(i) They are obtained in the large- N limit keeping t fixed, which is not uniform when $t \rightarrow 0$. However, the analysis of numerical results at finite N , obtained using the method based on the overlap matrix, shows that it is rapidly approached with increasing N , indeed $O(10^2)$ particles, or even less, are already sufficient to show it, see, e.g., Figs. 2-6.

(ii) They are obtained using only the completeness relation for the one-particle discrete spectrum of the $t = 0$ one-particle Hamiltonian. Therefore, these results do not depend on the particular form of the confining potential. The only essential ingredient is that it confines the particles within a strictly finite region of space. For example, it does not apply to a harmonic potential.

(iii) The entanglement entropies and particle variance show the same asymptotic relation already found in the

studies of the equilibrium ground-state properties [27], i.e.

$$S^{(\alpha)} \approx c_\alpha \pi^2 V, \quad (146)$$

which has been shown to be valid for the ground state of a large number of noninteracting Fermi particles, in any dimensions and for any subsystems, in homogeneous and nonhomogeneous conditions [27, 40].

Analogous results are obtained in the case only one wall of the initial trap drops, and the gas freely expands along one direction only. The essential point is that the resulting large- N two-point function corresponds to an appropriate continuum limit of the two-point function of lattice free fermions in the thermodynamic limit with boundaries. Therefore, one can derive asymptotic small- t expansions analogous to Eqs. (143-146) by using the known results for the asymptotic expansions of the entanglement entropies and particle cumulants in homogeneous systems with open boundary conditions, as shown in Sec. V.

The convergence to the large- N limit keeping fixed t is not uniform when $t \rightarrow 0$. This limit hides other scaling regimes at small times with $t \sim 1/N$ and $t \sim 1/N^2$, which are pushed toward the $t = 0$ axis when taking the large- N at fixed t . They emerge when studying the large- N limit keeping $\tau = Nt$ and $\theta \equiv N^2t$ fixed, as shown in Sec. IV. In particular, the large- N behavior keeping τ fixed, for sufficiently large τ ($\tau > 4/\pi$ for an interval equal to the original trap), is characterized by leading log behaviors analogous to those at equilibrium. On the other hand, the large- N scaling behavior at small τ ($\tau < 4/\pi$ for an interval equal to the original trap) remains unclear, deserving further investigation.

Another interesting physical case of nonequilibrium dynamics is that of a Fermi gas expanding from a harmonic trap, which is closer to the conditions of experiments with cold atoms, usually realized by trapping the atoms with an effective harmonic potential. The different initial conditions with respect to hard-wall traps give rise to different time dependences of the observables.

We investigate the unitary evolution of free fermion gases in time-dependent harmonic traps, described by the potential $V(x, t) = \frac{1}{2}\kappa(t)x^2$. We study the time dependence of one-particle observables, such as the particle density and its correlation functions, and observables associated with extended space regions around the center of the initial trap, such as the particle fluctuations and the entanglement entropies. The evolution in a time dependent harmonic trap, starting from the equilibrium ground state of a given initial trap with $\kappa_0 \equiv \kappa(0)$, show remarkable properties: the time dependence of all above-mentioned observables correspond to a global rescaling of the system size. For example, we prove that the Rényi entanglement entropy $S_Z^{(\alpha)}(x, t)$ of the interval $Z = [-x, x]$ (where $x = 0$ is the center of the original trap) has the time dependence

$$S_Z^{(\alpha)}(x, t) = S_Z^{(\alpha)}(x/s(t), 0) \quad (147)$$

where $s(t)$ is an analytical function of the time-dependent potential with $s(0) = 1$, and $S_Z^{(\alpha)}(x, 0)$ is the entanglement entropy of the interval $[-x, x]$ of the initial equilibrium state. In the case of a quantum quench with an instantaneous removal of the harmonic potential of frequency $\sqrt{\kappa_0}$, we have $s(t) = \sqrt{1 + \kappa_0 t^2}$. The entanglement entropy $S_B^{(\alpha)}(x, t)$ of any semi-infinite space $B = [-\infty, x]$ tend asymptotically to the initial half-space entanglement entropy, which is the half-space entanglement entropy of the ground state in a harmonic potential computed in Ref. [40], i.e.

$$\lim_{t \rightarrow \infty} S_B^{(\alpha)}(x, t) = S_B^{(\alpha)}(0, 0) \approx \frac{c_\alpha}{2} (\ln N + e_\alpha + \ln 2) \quad (148)$$

An analogous result applies to the particle cumulants. The large- N behavior of the time dependence of the entanglement entropy and particle fluctuations of the finite interval $Z = [-x, x]$, $S_Z^{(\alpha)}(x, t)$ and $V^{(m)}(x, t)$, can be easily determined using Eq. (147) and the large- N space dependence of the corresponding quantity at equilibrium [40], see Sec. V. In particular we consider an extended interval which contains (almost) all particles at $t = 0$ (apart from $O(1/N)$ corrections), and determine the large- N time dependence of its entanglement entropies and particle fluctuations. We find that the asymptotic large- N behaviors of the entanglement entropies and particle cumulants are characterized by the same leading logarithms at the equilibrium, and that relation (146) holds during the time evolution, except for very large times $t \gtrsim N$ where another regime sets.

Models of 1D noninteracting spinless Fermi gases have a wider application, because 1D Bose gases in the limit of strong short-ranged repulsive interactions can be mapped into a spinless fermion gas. The basic model to describe the many-body features of a boson gas confined to an effective 1D geometry is the Lieb-Liniger model with an effective two-particle repulsive contact interaction [31]. The limit of infinitely strong repulsive interactions corresponds to a 1D gas of impenetrable bosons [32], the Tonks-Girardeau gas. 1D Bose gases with repulsive two-particle short-ranged interactions become more and more nonideal with decreasing the particle density, acquiring fermion-like properties, so that the 1D gas of impenetrable bosons is expected to provide an effective description of the low-density regime of confined 1D bosonic gases [33]. Therefore, due to the mapping between 1D gases of impenetrable bosons and spinless fermions, some correlations in free fermion gases are identical to those of the hard-core boson gases, such as those related to the particle density, particle fluctuations of extended regions, and bipartite entanglement entropies of connected parts. Therefore, the results of this paper apply to 1D repulsively interacting Bose gases as well.

A further interesting issue, worth being investigated, concerns the universality of the behaviors found in this paper, whether some of them are shared with other many-body systems, in particular the small-time asymp-

otic behaviors of the entanglement entropies and particle fluctuations, which resembles universal behaviors found at equilibrium for systems with central charge $c = 1$. Another interesting issue concerns higher-dimensional systems, i.e. the time-dependence of the entanglement entropies during the expansion of gas released by the two or three-dimensional traps.

Acknowledgments

I thank Pasquale Calabrese and Mihail Mintchev for many useful discussions within common research projects.

Appendix A: Some analytic solutions for the one-particle problem in a time-dependent harmonic trap

We report some solutions of the Eq. (97).

(i) In the case of an instantaneous drop of the trap, so that $\kappa(t) = 0$ for $t > 0$,

$$s(t) = \sqrt{1 + \kappa_0 t^2}. \quad (\text{A1})$$

(ii) Instantaneous change to a confining potential with trap size l_f , so that $\kappa(t) = l_f^{-2}$ for $t > 0$,

$$s(t) = \sqrt{1 + (r^2 - 1) \left[\sin(\kappa_0^{1/2} t/r) \right]^2}, \quad (\text{A2})$$

where $r = l_f/l_0$.

(iii) Linear time dependence of the trapping potential [59], i.e. $\kappa(t) = \kappa_0 \tau$ and $\tau = 1 + t$,

$$s(t) = [\text{Re}W(\tau)]^{-1/2}, \quad \dot{s}(t) = -\frac{\text{Im}W(\tau)}{[\kappa_0 \text{Re}W(\tau)]^{1/2}}, \quad (\text{A3})$$

where the complex function $W(\tau)$ is the solution of the differential equation

$$iW' = \kappa_0^{1/2}(W^2 - \tau) \quad (\text{A4})$$

with $W(1) = 1$, which can be written as a combination of Airy functions,

$$W(\tau) = i\kappa_0^{-1/6} \frac{\text{Bi}'(-\kappa_0^{1/3} \tau) + c \text{Ai}'(-\kappa_0^{1/3} \tau)}{\text{Bi}(-\kappa_0^{1/3} \tau) + c \text{Ai}(-\kappa_0^{1/3} \tau)}, \quad (\text{A5})$$

$$c = -\frac{\kappa_0^{1/6} \text{Bi}(-\kappa_0^{1/3}) - i \text{Bi}'(-\kappa_0^{1/3})}{\kappa_0^{1/6} \text{Ai}(-\kappa_0^{1/3}) - i \text{Ai}'(-\kappa_0^{1/3})}.$$

(iv) Drop of the trap driven by a linear dependence:

$$\kappa(t) = 1 - t/t_d \quad \text{for } 0 \leq t \leq t_d, \quad (\text{A6})$$

$$\kappa(t) = 0 \quad \text{for } t > t_d.$$

where we set $\kappa(0) \equiv \kappa_0 = 1$. In this case the scaling function $s(t)$ is given by

$$s(t) = [\text{Re}W(1 - t/t_d)]^{-1/2} \quad \text{for } 0 \leq t \leq t_d, \quad (\text{A7})$$

and

$$s(t) = \sqrt{a + b(t - t_d) + c(t - t_d)^2} \quad \text{for } t > t_d, \quad (\text{A8})$$

with

$$c = \frac{4 + b^2}{4a}, \quad (\text{A9})$$

$$a = s(t_d)^2 = 1.3067374\dots, \quad (\text{A10})$$

$$b = 2s(t_d)s'(t_d) = \frac{0.90519789\dots}{t_d} \quad (\text{A11})$$

-
- [1] E.A. Cornell and C.E. Wieman, Rev. Mod. Phys. 74, 875 (2002).
[2] N. Ketterle, Rev. Mod. Phys. 74, 1131 (2002).
[3] I. Bloch, J. Dalibard, and W. Zwerger, Rev. Mod. Phys. 80, 885 (2008).
[4] A. Polkovnikov, K. Sengupta, A. Silva, and M. Vengalattore, Rev. Mod. Phys. 83, 863 (2011).
[5] A. del Campo, G. Garca-Calderon, and J.G. Muga, Phys. Rep. 476, 1 (2009).
[6] P. Ohberg and L. Santos, Phys. Rev. Lett. 89, 240402 (2002).
[7] P. Pedri, L. Santos, P. Ohberg, and S. Stringari, Phys. Rev. A 68, 043601 (2003).
[8] A. Minguzzi and D.M. Gangardt, Phys. Rev. Lett. 94, 240404 (2005).
[9] M. Rigol and A. Muramatsu, Phys. Rev. Lett. 94, 240403 (2005).
[10] A. del Campo and J.G. Muga, EPL 74, 965 (2006).
[11] D.M. Gangardt and M. Pustilnik, Phys. Rev. A 77, 041604 (2008).
[12] P. Calabrese and J. Cardy, J. Phys. A 42, 504005 (2009).
[13] I. Peschel and V. Eisler, J. Phys. A 42, 504003 (2009).
[14] P. Calabrese and J. Cardy, J. Stat. Mech. P10004 (2007).
[15] V. Eisler and I. Peschel, J. Stat. Mech. P06005 (2007).
[16] A.M. Lauchli and C. Kollath, J. Stat. Mech. P05018 (2008).
[17] V. Eisler, D. Karevski, T. Platini, and I. Peschel, J. Stat. Mech. P01023 (2008).
[18] M. Fagotti and P. Calabrese, Phys. Rev. A 78, 010306 (2008).
[19] I. Klich and L. Levitov, Phys. Rev. Lett. 102, 100502 (2009).
[20] B. Hsu, E. Grosfeld, and E. Fradkin, Phys. Rev. B 80, 235412 (2009).
[21] J.-M. Stephan and J. Dubail, J. Stat. Mech. P08019 (2011).
[22] J. Cardy, Phys. Rev. Lett. 106, 150404 (2011).
[23] I. Klich, G. Refael, and A. Silva, Phys. Rev. A 74, 032306

- (2006).
- [24] H.F. Song, S. Rachel, and K. Le Hur, Phys. Rev. B 82, 012405 (2010).
- [25] H.F. Song, C. Flindt, S. Rachel, I. Klich, and K. Le Hur, Phys. Rev. B 83, 161408 (2011).
- [26] H.F. Song, S. Rachel, C. Flindt, I. Klich, N. Laflorencie, and K. Le Hur, Phys. Rev. B 85, 035409 (2012).
- [27] P. Calabrese, M. Mintchev, and E. Vicari, EPL 98, 20003 (2012).
- [28] L. Amico, R. Fazio, A. Osterloh, and V. Vedral, Rev. Mod. Phys. 80, 517 (2008).
- [29] J. Eisert, M. Cramer, and M.B. Plenio, Rev. Mod. Phys. 82, 277 (2010).
- [30] S. Sachdev, *Quantum Phase Transitions* (Cambridge Univ. Press, 1999).
- [31] E.H. Lieb and W. Liniger, Phys. Rev. 130, 1605 (1963).
- [32] M. Girardeau, J. Math. Phys. (N.Y.) 1, 516 (1960); M.D. Girardeau, Phys. Rev. 139, B500 (1965).
- [33] D.S. Petrov, G.V. Shlyapnikov, and J.T.M. Walraven, Phys. Rev. Lett. 85, 3745 (2000).
- [34] T. Kinoshita, T. Wenger, and D.S. Weiss, Nature 440, 900 (2006).
- [35] T. Kinoshita, T. Wenger, and D.S. Weiss, Science 305, 1125 (2004); Phys. Rev. Lett. 95, 190406 (2005).
- [36] T. Stöferle, H. Moritz, C. Schori, M. Köhl, and T. Esslinger, Phys. Rev. Lett. 92, 130403 (2004).
- [37] B. Paredes, A. Widera, V. Murg, O. Mandel, S. Fölling, I. Cirac, G. Shlyapnikov, R.W. Hänsch, and I. Bloch, Nature 429, 277 (2004).
- [38] B. Laburthe Tolra, K.M. O'Hara, J.H. Huckans, S.L. Rolston, and J.V. Porto, Phys. Rev. Lett. 92, 190401 (2004).
- [39] S. Hofferberth, I. Lesanovsky, B. Fischer, T. Schumm, and J. Schmiedmayer, Nature 449, 324 (2007).
- [40] E. Vicari, arXiv:1204.2155.
- [41] S. Godoy, Phys. Rev. A 65, 042111 (2002).
- [42] A. del Campo and J.G. Muga, J. Phys. A 38, 9802 (2005).
- [43] E. Lukacs, *Characteristic functions* (C. Griffin, London 1970).
- [44] B-Q Jin and V.E. Korepin, J. Stat. Phys. 116, 79 (2004).
- [45] P. Calabrese, M. Mintchev, and E. Vicari, Phys. Rev. Lett. 107, 020601 (2011).
- [46] P. Calabrese, M. Mintchev, and E. Vicari, J. Stat. Mech. P09028 (2011).
- [47] P. Calabrese, M. Mintchev, and E. Vicari, EPL 97, 20009 (2012).
- [48] P. Calabrese, M. Mintchev, and E. Vicari, J. Phys. A 45, 105206 (2012).
- [49] A. del Campo, Phys. Rev. A 84, 012113 (2011).
- [50] L.D. Landau and L.M. Lifshitz, *Quantum Mechanics Non-Relativistic Theory*, Pergamon Press, 1977.
- [51] P. Calabrese and J. Cardy, J. Stat. Mech. P06002 (2004).
- [52] P. Calabrese, M. Campostrini, F.H.L. Essler, and B. Nienhuis, Phys. Rev. Lett. 104, 095701 (2010); P. Calabrese and F.H.L. Essler, J. Stat. Mech. P08029 (2010).
- [53] M. Fagotti and P. Calabrese, J. Stat. Mech. P01017 (2011).
- [54] Yu. Kagan, E.L. Surkov, and G.V. Shlyapnikov, Phys. Rev. A 54, R1753 (1996).
- [55] M.D. Girardeau and E.M. Wright, Phys. Rev. Lett. 84, 5691 (2000).
- [56] V.S. Popov and A.M. Perelomov, Sov. Phys. JETP 30, 910 (1970).
- [57] F. Kalish and D. Braak, J. Phys. A 35, 9957 (2002).
- [58] T.M. Garoni, P.J. Forrester, and N.E. Frankel, J. Math. Phys. 46, 103301 (2005).
- [59] M. Campostrini and E. Vicari, Phys. Rev. A 82, 063636 (2010); Phys. Rev. A 81, 063614 (2010).